



Article

Tracking Land-Use and Land-Cover Change Through Fragmentation Dynamics in the Ciliwung River Watershed, Indonesia: A Remote-Sensing and GIS Approach

Rezky Khrisrachmansyah 1,20, Paul Brindley 1,*0, Nicola Dempsey 10 and Tom Wild 10

- School of Architecture and Landscape, The University of Sheffield, Sheffield S10 2TN, UK; rkhrisrachmansyah1@sheffield.ac.uk (R.K.); n.dempsey@sheffield.ac.uk (N.D.); t.wild@sheffield.ac.uk (T.W.)
- ² Landscape Architecture Department, IPB University, Bogor 16680, Indonesia
- * Correspondence: p.brindley@sheffield.ac.uk

Abstract

Understanding landscape fragmentation is crucial to explore comprehensive land-useland-cover (LULC) change within fast-growing urbanisation. While LULC change is a global concern, limited research explores landscape fragmentation along river and road infrastructure in high-density riverine contexts. This study addresses this gap through understanding dynamic landscape fragmentation patterns to track LULC in the Ciliwung River, Indonesia, from 1990 to 2020. The research employed remote sensing, GIS, R programming with Landsat data, Normalised Difference Vegetation Index (NDVI) values, buffering, and landscape metrics. The findings show minimal fragmentation was concentrated downstream near Jakarta, while significant fragmentation, manifesting as green loss, occurred in the midstream. Buffer analysis showed high green loss in the upstream segment both near the river and roads, particularly within a 0-400 m buffer. However, landscape metrics identified changes in the midstream close to the river buffer (0-200 m) indicating that riparian green spaces in this area persist as relatively large but ecologically unconnected "chunks". The stability of these remaining patches makes them a crucial asset for targeted restoration. These findings contribute to a deeper understanding of how river and road networks influence the change, highlighting the integral role of remote sensing and GIS in monitoring LULC change for natural preservation.

Keywords: landscape fragmentation; remote sensing; GIS; LULC change; high-density riverine; Normalised Difference Vegetation Index (NDVI)



Academic Editor: Martin Boltiziar

Received: 10 September 2025 Revised: 17 October 2025 Accepted: 21 October 2025 Published: 25 October 2025

Citation: Khrisrachmansyah, R.; Brindley, P.; Dempsey, N.; Wild, T. Tracking Land-Use and Land-Cover Change Through Fragmentation Dynamics in the Ciliwung River Watershed, Indonesia: A Remote-Sensing and GIS Approach. *Land* 2025, 14, 2127. https://doi.org/ 10.3390/land14112127

Copyright: © 2025 by the authors. Licensee MDPI, Basel, Switzerland. This article is an open access article distributed under the terms and conditions of the Creative Commons Attribution (CC BY) license (https://creativecommons.org/licenses/by/4.0/).

1. Introduction

Rapid urban agglomeration driven by megacities such as Jakarta (Indonesia) impacts landscape patterns, including land-use and land-cover (LULC) changes, fragmentation changes, and environmental and ecological degradation [1–3]. Rivers across these megacities are vital as a source of water but also pose challenges due to competition and conflict between urban and rural users [4]. The anthropogenic pressure in megacities intensifies land fragmentation into more complex patterns and degrades green cover spaces of urban nature, affecting human health [5–7].

Landscape fragmentation is the breaking apart of natural land cover(s) into smaller areas, thus influencing biophysical and human movement and distribution [8,9]. Landscape fragmentation in riverine areas presents significant challenges that need to be explored and understood.

Land 2025, 14, 2127 2 of 29

Research in the past few decades has demonstrated that land fragmentation affects habitat quality and ecosystem structure and function [10]. Studies suggest that fragmentation can provide opportunities for corridor connectivity, conservation, and ecological enhancement [11]. Rivers, as essential landscape elements, possess unique ecological value and are dynamic ecosystems due to continuous changes [12,13]. They also form important networks contributing to urban ecological connectivity [14,15].

Urbanisation is further accelerated by the development of transportation infrastructure, which influences land fragmentation in urban–rural areas [16–18]. Road infrastructure in developing countries, as well as in megacities, is highly dynamic [19,20]. One of the main causes leading to land fragmentation is the development of road infrastructure [21]. This point is further supported by recent research from Ding et al. [22], which employed an ecological network approach to demonstrate that construction land expansion, including roads (in both urban and rural areas), significantly contributes to habitat isolation leading to ecological degradation.

Road infrastructure networks are an established driver of fragmentation, with high-impact linear features, such as highways, causing severe habitat loss and landscape degradation, particularly evident within a 1000 m buffer zone surrounding the infrastructure [23]. On the other hand, riparian area fragmentation is known to directly influence aquatic health. Yirigui et al. [24] demonstrated that the negative impact of riparian forest fragmentation on ecological communities, including diatoms, macroinvertebrates, and fish, was strongly correlated with the proximity of fragmentation to the stream, rather than distance across the entire watershed. This highlights a dual concern for landscape planning and management, addressing the broad, systemic fragmentation caused by major roads and the highly sensitive, localised fragmentation within close-range river buffers.

The recent literature focused on landscape fragmentation in megacities, particularly through landscape metrics, employs remote-sensing (RS) and GIS approaches to provide critical insights into the dynamics of urban expansion. The primary implication highlighted in studies across Asia, including Dhaka and Xi'an, is the severe ecological fragmentation and environmental degradation resulting from rapid urban sprawl, particularly in sensitive urban fringe areas [3,25]. This fragmented characteristic of the urban fringe is directly relevant to understanding fragmentation patterns because upstream and midstream/transition zones can act as fringe areas separate from downstream urban centres. This degradation is driven by relevant factors, including high urban expansion intensity and irregular, uneven sprawl as found in Dhaka [3,25]. The application of this approach offers key advantages, enabling the detailed analysis of spatiotemporal dynamics of fragmentation, focusing on broad land-use changes [25]. Studies have begun to explore the societal controversies and broader implications of physical fragmentation, such as the relationship between ecological fragmentation and the fragmentation of spatial governance in the urban fringe. This suggests that the effective management of these complex areas remains a significant challenge for sustainable development in cities [3].

Furthermore, the imperative for action extends to future and broader policy. For example, Struebig et al. [26] argues that addressing the biodiversity crisis and socioeconomic realities in rapidly developing Southeast Asian countries requires a comprehensive policy–practice decision-making framework. This necessitates innovative landscape conservation technologies, community-led management, nature-based climate solutions, and international sustainability commitments to ecosystem restoration, alongside biodiversity protection, and climate mitigation. Satellite image analysis is crucial for mapping LULC changes and understanding fragmentation. LULC monitoring tracks land-use changes and their environmental impacts. The Normalised Difference Vegetation Index (NDVI) provides an efficient alternative to complex LULC classification due to readily available

Land 2025, 14, 2127 3 of 29

satellite data, offering insights into human—environment interactions [27,28]. Ultimately, the use of remote-sensing (RS) and GIS approaches is therefore vital to explore the dynamic and unique characteristics of megacities and their transition zones, providing a crucial foundation for effective future monitoring, policy development, and overcoming these broader complexities and challenges.

In the Jakarta megacity and its fringe areas, collectively known as Jabodetabek (Jakarta, Bogor, Depok, Tangerang, and Bekasi), the expansion of road infrastructure has driven the growth of settlement areas along the Ciliwung River. This phenomenon has impacted the natural environment, including a reduction in green and natural areas (including forest and dense vegetation) which in turn has increased the occurrence of floods and landslides [29,30].

However, there is limited systematic research on how the interplay between rivers and road transportation affects fragmentation changes in the context of riverine megacities. Furthermore, there is a need for studies tracking land-use/land-cover (LULC) changes and associated holistic challenges [31,32]. This approach is necessary because while developments along rivers and roads have occurred as settlements have developed, few studies explicitly separate out fragmentation, and the ensuing ecological impact, related to these linear features.

This study aims to deepen the understanding of landscape fragmentation by examining varying fragmentation patterns in urban and rural riverine contexts using RS and GIS approaches. The visionary aspect of this study lies in examining the interplay between rivers and roads by questioning how and where fragmentation changes occur along this linear infrastructure in a highly populous city, particularly in a megacity context. This includes an adjacent focus on LULC changes to inform future environmental, ecological, and natural resource preservation efforts.

Specifically, the objectives of this paper are to analyse the differential pattern of linear landscape features (the riverine corridor and major road networks) on landscape fragmentation changes across the urban–rural continuum of the megacity and its surrounding area, particularly focusing on the Ciliwung River. Second, the paper seeks to track LULC changes, by applying an integrated methodology using spatial—temporal remote-sensing data, GIS buffering techniques, and landscape metrics in a highly dense, dynamic riverine context. The paper will therefore provide empirical evidence to inform proactive land-use planning, environmental regulation, and targeted ecological preservation strategies for river corridors facing rapid urbanisation pressures.

2. Materials and Methods

The material of this study was Landsat imagery with a spatial resolution of 30 m. The near-infrared and red spectral bands were selected for the NDVI calculation. To assess changes over the study period, a dataset containing images from 9 July 1990 for 1990 data and 22 April and 24 May 2020 for 2020 data was used. The 1990 and 2020 data were acquired on 20 April 2022.

The methodology utilises remote sensing, GIS, and R programming, employing NDVI values, buffer analysis, and landscape metrics. The NDVI is a common remote-sensing tool for quantifying fragmentation [33]. As an indicator of vegetation health, it reflects ecosystem degradation through the decline of green cover [34]. It can also differentiate between water bodies, built-up areas, and vegetation, enabling it to calculate fragmentation metrics.

Land 2025, 14, 2127 4 of 29

The analysis is enriched by a diverse set of landscape fragmentation metrics as previously outlined, including NP, ED, Contag, and diversity indices, to provide a multi-scalar perspective on structural change [35]. The integration of NDVI change detection with this fragmentation analysis, specifically linked to buffer analysis of rivers and roads, enables the research to provide an ecologically meaningful explanation of how human-induced disturbances impact the watershed's structure, governing services like flood control and water quality regulation.

Further details of the process are explained later in Section 2.2.1 for the NDVI calculation methodology and Section 2.2.2 for the buffer analysis and metrics calculation.

2.1. Study Area

The case study is located in the Ciliwung River area, Indonesia, within the Geographic Coordinate System of WGS 1984, UTM Zone 48S, and its watershed. This location was selected because it is situated in a megacity with a high population density and significant road infrastructure development.

The Ciliwung watershed, spanning 13 cities within Jabodetabek (Figure 1), lies at the interface of the Western Java rain and montane rain forests [36] with Bogor City resting within this transition zone. Formerly a Jakarta hinterland, Bogor's rapid growth has caused substantial LULC configuration change, with urban expansion and green and water loss, leading to surface urban heat island and significant urban–rural fragmentation [37,38].

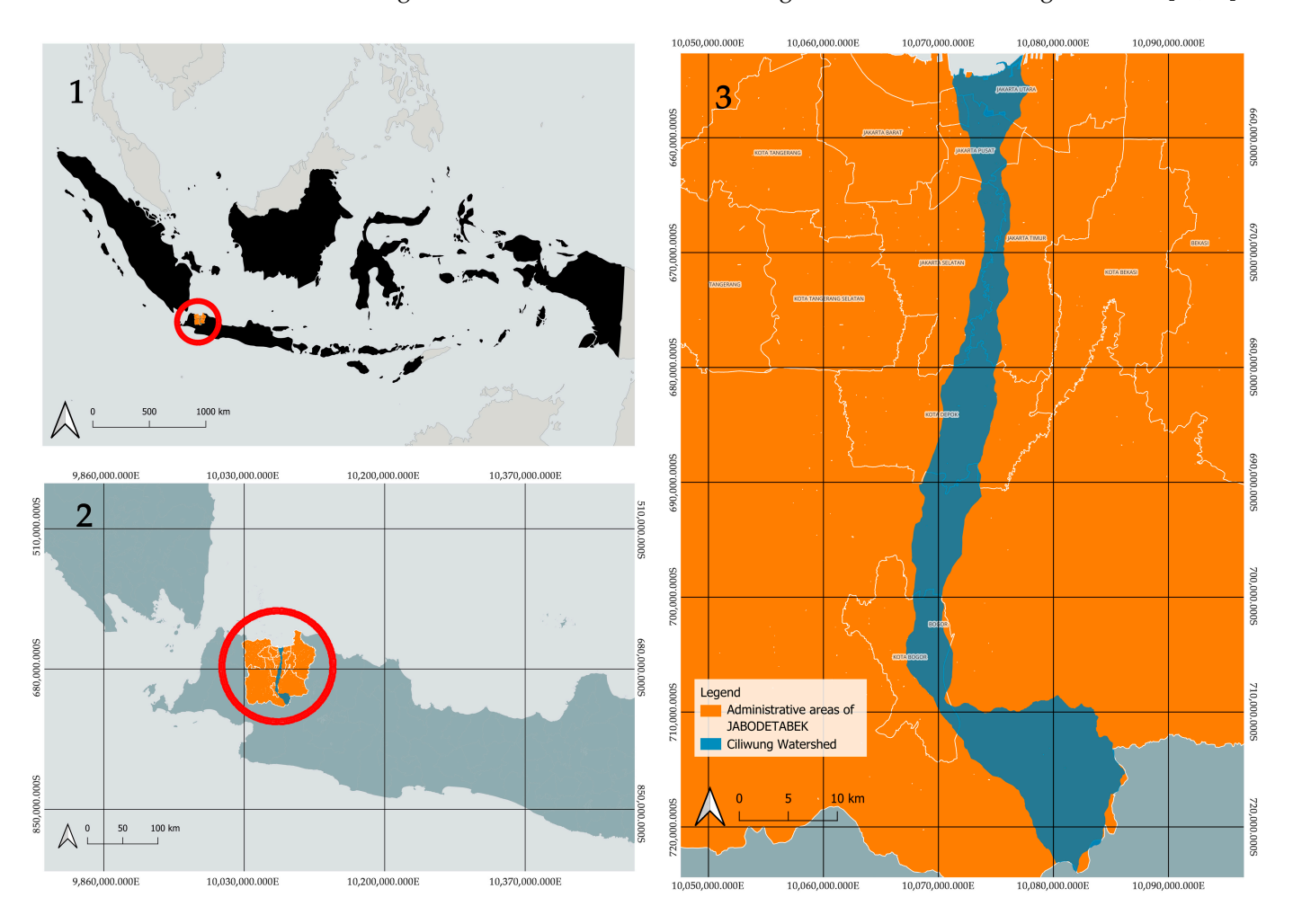


Figure 1. Map of Indonesia (1); Map of Jakarta–Bogor–Depok–Tangerang–Bekasi (Jabodetabek) (2); Map of Ciliwung watershed (3). The red circle shows the location of the study area.

Land **2025**, 14, 2127 5 of 29

2.2. Methodology

This study utilised Landsat 5 and 8 satellite imagery, sourced from the USGS (https://earthexplorer.usgs.gov (accessed on 20 March 2022)). This research chose Landsat due to it being commonly used and to ensure rigour and comparability [39,40].

2.2.1. NDVI Calculation

The methodology utilised NDVI values for a 30-year temporal comparison (1990–2020). Data acquisition focused on the optimal summer months (April to July), with the clearest cloud coverage single-day image selected for each year. This research calculated the NDVI maps considering values greater than 0.25 as indicative of green areas following the work of Wang et al. [41]. Research by Liu et al. [42] reinforces this principle, noting that in pan-tropical regions, NDVI values greater than 0.25 typically correspond to forests, dense vegetation, and grassland, thus excluding most bare land and built-up areas.

NDVI focuses on green areas (forests, plantations, agriculture, etc.) to distinguish vegetated from non-vegetated areas [43]; this research used NDVI because it is a widely used and well-established index for vegetation identification [44]. It utilises two spectral bands from satellite imagery: red and near-infrared bands; in this research, we use Landsat 5 using Band 4 (near-infrared) and Band 3 (red) for 1990, and Landsat 8 using Band 5 (near-infrared) and Band 4 (red) for 2020. The formula of NDVI can be seen below:

$$NDVI = (NIR - R)/(NIR + R)$$

After obtaining these values, this research used ArcMap 10.7.1 to calculate changes over time using map algebra and the raster calculator with Python expressions (version 2.7.16). This research classified the values into four classes: areas of vegetation loss; non-vegetated areas (indicative of built-up areas); stable green areas; and areas with increased vegetation or greening.

The Ciliwung watershed was divided into three segments based on administrative boundaries: upstream, midstream (or transition), and downstream. Maps were generated to show the location of green areas in both 1990 and 2020. This step was conducted using a raster calculator, map algebra, in ArcGIS (version ArcMap 10.7.1).

The next step was to understand the fragmentation changes within the watershed boundary. This step involved using buffer analysis to examine fragmentation phenomena, with distance buffers of both the rivers and main roads.

A further step was the landscape fragmentation analysis, which was conducted using the R programming language within R-Studio (version RStudio 2024.04.2+764) to track LULC changes. Landscape fragmentation was assessed using metrics including total class area (CA), percentage of landscape (PL), number of patches (NP), Shannon's diversity index (SHDI), Simpson's diversity index (SIDI), contagion (Contag), and edge density (ED) [35].

This study focuses on five landscape metrics, NP, Contag, ED, SHDI, and SIDI, which are crucial considerations for understanding the pattern of landscape fragmentation and its ecological context. NP quantifies the total count of distinct, separate patches or islands or chunks of a specific land-cover type. For instance, a homogeneous landscape with only one continuous forest block has NP = 1. If that forest is split into ten smaller pieces or patches, NP = 10.

Land 2025, 14, 2127 6 of 29

Contagion measures landscape aggregation, where high contagion indicates a few large, clumped patches that tend to stick together and form continuous blocks. This generally indicates a simpler, less fragmented landscape structure. Conversely, low contagion suggests a fragmented landscape with many patches that are small, scattered, and mixed up. Edge density (ED) measures the total length of internal patch boundaries per unit area, providing a measure of landscape complexity; high ED signifies a complex, fragmented landscape, while low ED indicates a simple landscape with large, uniform areas. Contagion and ED are inversely related: high ED (many borders between different patch types) correlates with low contagion (high fragmentation), and vice versa.

Shannon's diversity index and Simpson's diversity index are both statistical measures of biological diversity that measures species richness, with higher values indicating greater diversity and complex mix where no single land-cover type completely dominates the area. While Simpson's index focuses on species dominance and is less sensitive to rare species, Shannon's index is more sensitive to species richness and the evenness of distribution among all species. By combining the calculations from these five metrics, this study generates a comprehensive picture of the landscape's structure, identifying the variety and spatial distribution of the natural landscape within the urban–rural riverine [35]. Additional detail around these metrics and their measurement can be found in Appendix B.

The formula of the fragmentation metrics used in this study can be seen in Appendix B. These were calculated using the "landscapemetrics" package in R (https://cran.r-project.org/web/packages/landscapemetrics/landscapemetrics.pdf (accessed on 31 March 2025) and related R spatial packages. The research framework is depicted below (Figure 2).

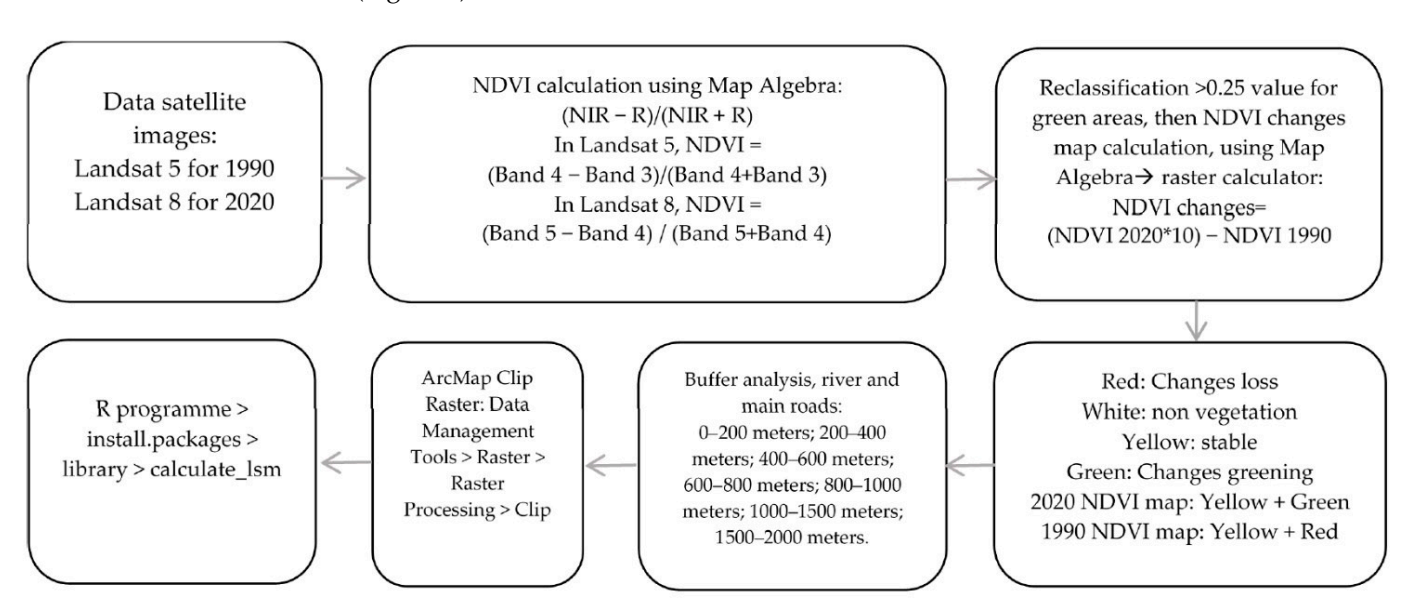


Figure 2. Framework of the study. The arrows illustrate the sequential phases and workflow from data preparation to the final analysis.

Land **2025**, 14, 2127 7 of 29

The chosen suite of indices provides a targeted assessment of landscape health and change in the rapidly developing Ciliwung watershed. The foundation of this analysis is the NDVI, which functions as a robust proxy for photosynthetic activity and biomass density. A decline in NDVI, particularly in areas classified as vegetation loss or non-vegetated (built-up areas), directly quantifies the loss of critical ecological functions. These vital functions, such as carbon sequestration, hydrological regulation (stormwater control), and the mitigation of soil erosion vulnerability, are essential for maintaining the watershed's resilience against intense urban pressures. By using NDVI to measure the conversion to non-vegetated areas, the study directly tracks the impact of urban encroachment, identifying it as a central and quantifiable pressure point.

2.2.2. Buffer Analysis and Metrics Calculation

This study explored varying fragmentation using the watershed boundary. This research employed buffer distances of 0–200 m, 200–400 m, 400–600 m, 600–800 m, 800–1000 m, 1000–1500 m, and 1500–2000 m. The buffers generation is illustrated in Figure 3 and the output buffers for both the river and road are shown in Figure 4. This study, however, focuses on major or main road infrastructure, including primary roads, national roads, and highways. This is due to the availability of data and ability to compare it with the development of roads narrower than the core main roads. The buffer analysis was conducted using ArcMap 10.7.1. through the Buffer tool. Each raster buffer area was calculated using R Programming (version RStudio 2024.04.2+764) to determine the NP, Contag, ED, SHDI, and SIDI.

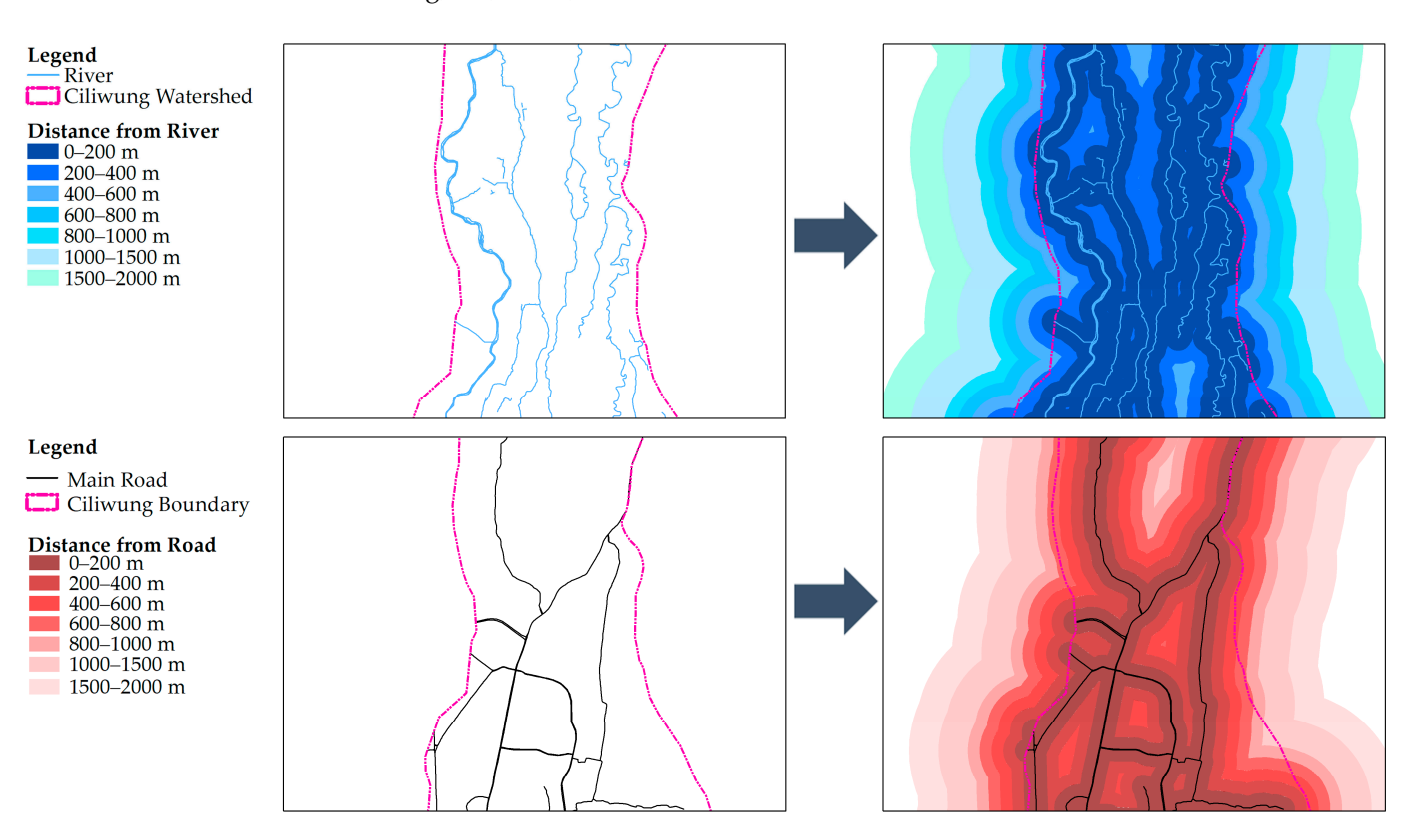


Figure 3. Buffer analysis: for the river (**top**) and main roads (**bottom**) showing original input (**left**) and buffered output (**right**). The arrows illustrate the derivation of buffer zones from the primary river and main road networks.

Land 2025, 14, 2127 8 of 29

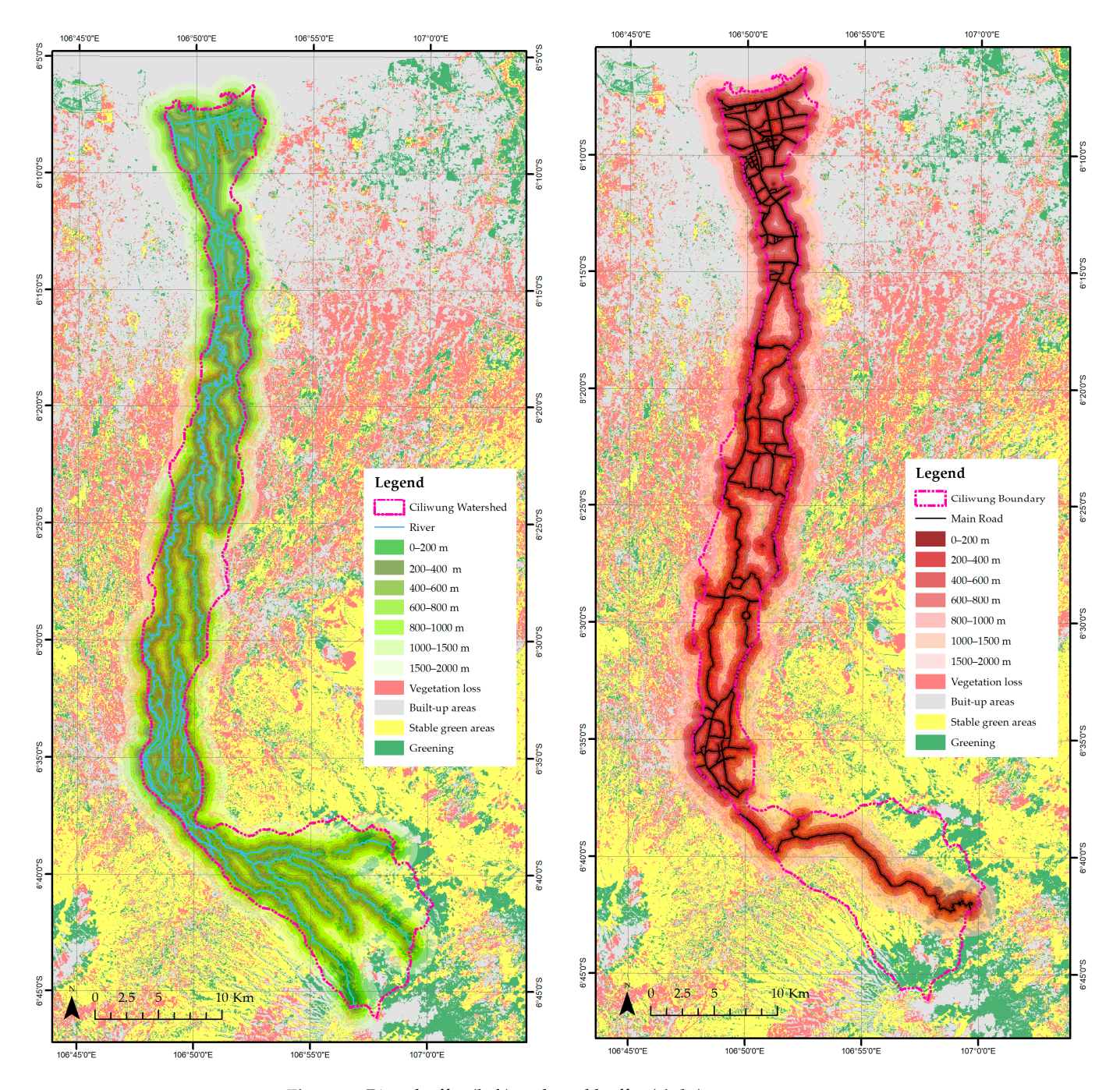


Figure 4. River buffer (left) and road buffer (right).

3. Results and Discussion

3.1. Results

The NDVI calculations (Figure 5) found significant fragmentation changes in transitional areas, accounting for 38% of the watershed, which includes Bogor City and Bogor Regency. Non-green spaces, mostly located in the downstream areas around the capital city Jakarta and Depok City, were less fragmented and accounted for approximately 64% of the total watershed area. In the upstream area, stable conditions prevailed, covering around 55% of the total watershed, primarily linked to plantation areas. However, there was also considerable greening in upstream areas, which constitute about 24% of the watershed (Figure 5).

Land **2025**, 14, 2127 9 of 29

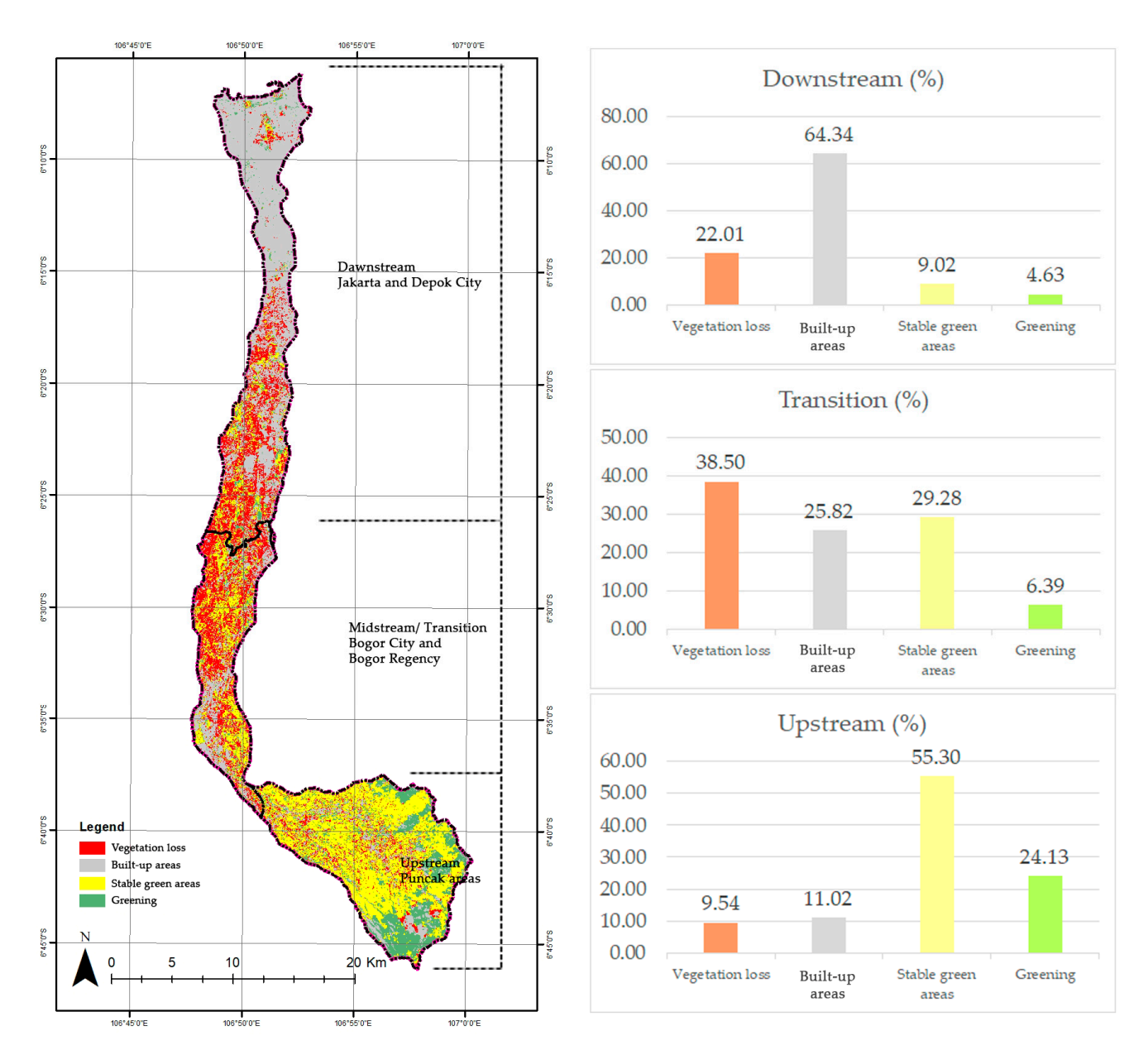


Figure 5. NDVI changes (left); and statistics of the NDVI change within river segments (right).

3.1.1. Fragmentation (Based on NDVI) Changes Across the River and Road Buffer

Buffer analysis based on NDVI changes reveals that fragmentation changes occur differently among the upstream, midstream, and downstream sections of the river. As shown in Table 1, for the upstream river buffer, green loss occurs most significantly in the under 200 m and 200–400 m buffers, with both having 12% of the buffer recorded as areas of green loss compared to a gradual decrease to 8% green loss coverage as the distance from the river increases to 2000 m. The amount of loss within the midstream was much greater than upstream and with a different geography. Here, in the midstream, green loss is highest within the 400–600 m buffer at 45% of the buffer area. Conversely, the lowest green loss in the midstream is found in the 200 m buffer, at 31%. Downstream, the trend is similar to upstream, with green loss being most pronounced near the river (32% at 200 m) and then decreasing with distance. Overall, the highest rate of building change across all segments is downstream within the 1000–2000 m buffer, reaching 75%. This suggests that while green loss occurs highly in the midstream of the Ciliwung River, green areas still remain very close to the river in this segment (30% stable green at 200 m).

Table 1. River buffer table, % of fragmentation changes from 1990 to 2020.

Upstream	0–200 m	200–400 m	400–600 m	600–800 m	800–1000 m	1000–1500 m	1500–2000 m
Green Lost	12	12	11	10	10	9	8
Non-Green (stable building)	14	12	11	9	11	10	9
Stable green	52	58	57	58	57	58	59
Greening	22	19	22	23	22	23	24
Total %	100	100	100	100	100	100	100
Midstream	0–200 m	200–400 m	400–600 m	600–800 m	800–1000 m	1000–1500 m	1500–2000 m
Green Lost	31	44	45	44	42	40	40
Non-Green (stable building)	32	27	24	26	25	24	24
Stable green	30	23	24	23	27	31	32
Greening	8	6	7	7	6	5	4
Total %	100	100	100	100	100	100	100
Downstream	0–200 m	200–400 m	400–600 m	600–800 m	800–1000 m	1000–1500 m	1500–2000 m
Green Lost	32	30	26	23	19	14	13
Non-Green (stable building)	46	58	62	64	69	75	75
Stable green	17	9	8	8	7	6	5
Greening	5	3	3	4	5	5	6
Total %	100	100	100	100	100	100	100

However, fragmentation changes near main roads (Table 2) show a different trend. They are most pronounced within the 1000–2000 m buffer, with a green loss of around 70% in the midstream at 1500–2000 m and downstream at 1500–2000 m. The highest green loss is at 71% in the midstream and 69% downstream, both in the 1500–2000 m buffer. In Appendix A, Figures A1 and A2 show the graphs for both the river and road buffers.

Table 2. Road buffer table, % of fragmentation changes from 1990 to 2020.

Upstream	0–200 m	200–400 m	400–600 m	600–800 m	800–1000 m	1000–1500 m	1500–2000 m
Green Lost	15	16	13	16	15	11	9
Non-Green (stable building)	28	13	11	11	10	8	7
Stable green	45	54	58	58	59	64	66
Greening	12	17	17	16	16	17	19
Total %	100	100	100	100	100	100	100
Midstream	0–200 m	200–400 m	400–600 m	600–800 m	800–1000 m	1000–1500 m	1500–2000 m
Green Lost	35	35	41	39	44	43	71
Non-Green (stable building)	37	29	19	17	13	10	12
Stable green	21	29	34	38	37	42	16
Greening	7	7	6	6	6	6	1
Total %	100	100	100	100	100	100	100
Downstream	0–200 m	200–400 m	400–600 m	600–800 m	800–1000 m	1000–1500 m	1500–2000 m
Green Lost	14	22	27	30	39	36	69
Non-Green (stable building)	76	64	57	54	47	37	13
Stable green	6	10	12	11	10	19	15
Greening	5	4	5	5	5	7	4
Total %	100	100	100	100	100	100	100

Downstream, areas closer to the main roads (under 200 m) have a lower green loss (14%) compared to the further buffers. Even though the overall trend is similar in the midstream, there is a slight difference where green loss decreases within the 600–800 m

buffer (39%) before increasing again to 44% in the 800–1000 m buffer. Upstream, the pattern is less consistent, with a high fragmentation change (16% green loss) occurring within the 200–400 m and 600–800 m buffers before decreasing after 1000 m. Therefore, fragmentation changes occur highly near the main road upstream, while in the midstream and downstream they are more pronounced at distances over 1000 m from the main roads.

3.1.2. Landscape Metrics Across the River and Road Buffers Upstream River Buffer

The river buffer fragmentation analysis reveals changes in the upstream Ciliwung River. Based on Figure 6, in 1990 and 2020, the NP initially increased before gradually decreasing across most buffer zones, from under 200 m to 2000 m. Notable exceptions to this trend include a decline in patch numbers within the 200–400 m zone in 1990, and the 600–800 m zone in 2020 (see Figure 6a,b). The largest drops in NP were observed in the 1000–1500 m and 1500–2000 m zones. While the patches that occurred within the 400–600 m buffer zones (at 24% NP) remained stable in both years, the highest change in NP was a 4% increase within the 200–400 m zone (Figure 6c).

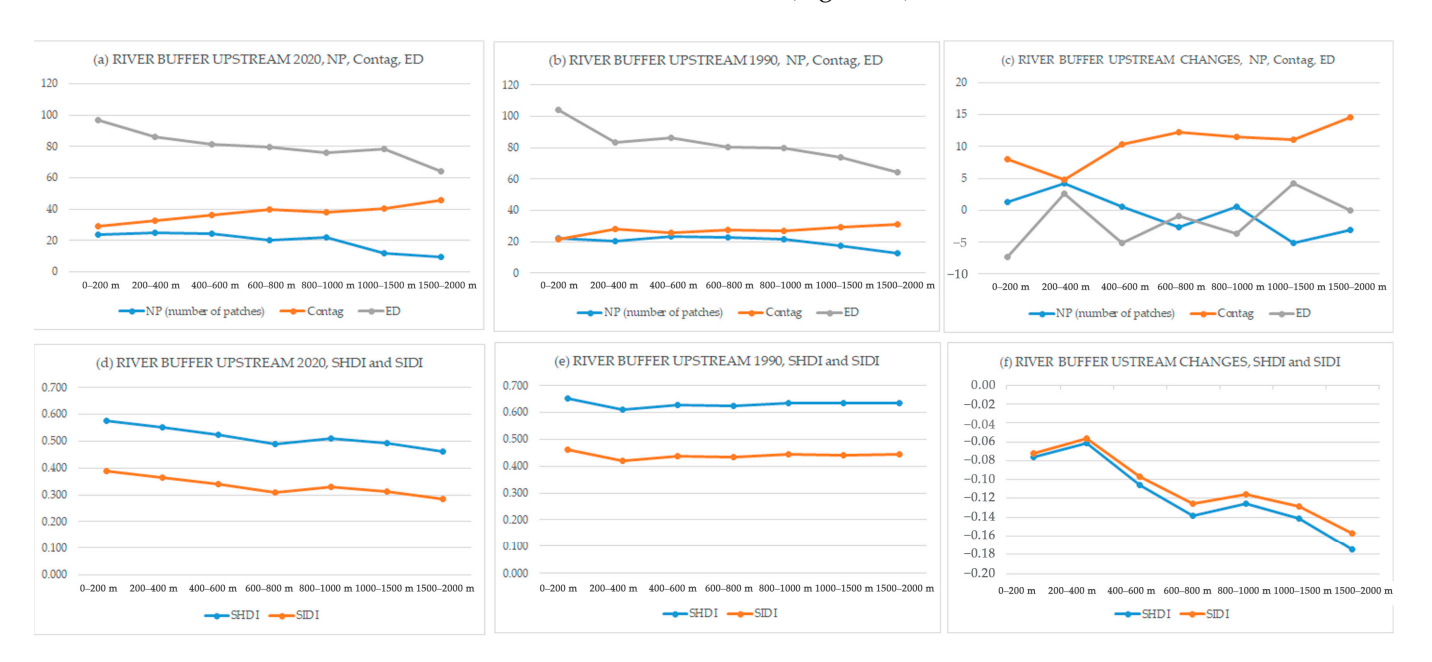


Figure 6. Upstream river buffer graphs.

Contag and ED results show opposite trends, as expected. A higher Contag value indicates greater connectivity, while a higher ED value suggests more fragmentation or "patchiness". In both 1990 and 2020, the ED generally decreased as the distance from the river increased, suggesting that areas closer to the river are more fragmented. Conversely, the Contag index tended to increase with distance, indicating higher aggregation or connectivity further from the river (see Figure 6a,b). The most significant change in Contag occurred within the 1500–2000 m zone, where a positive value means an increase in contagion. The ED changes were most pronounced in the under 200 m zone, which is a negative value, meaning a decrease in ED or more aggregation or less fragmentation than before (see Figure 6c). An unusual condition was observed in the 1000–1500 m zone, where the ED change was at its positive peak, suggesting the area became more fragmented (Figure 6c). This indicates substantial shifts in this zone over the 30-year period.

In terms of diversity indices, the SHDI and SIDI show similar patterns. In 1990, there was no significant difference in diversity across the buffer zones, except for a drop within the 200–400 m buffer. However, in 2020, diversity consistently decreased from the 200 m to

the 2000 m buffer zones (see Figure 6d,e). This decline is most pronounced in the change data, which shows a significant drop in both SHDI and SIDI from areas near the river to those furthest away, meaning there was a decline in diversity from 1990 to 2020 (see Figure 6f). The highest change in diversity occurred in the 200–400 m zone, correlating with the highest change in NP in this area.

The table for the river buffer changes within the upstream area can be seen in Appendix A, Table A1.

Midstream River Buffer

Based on the data and graphs of Figure 7, the analysis of the midstream section of the river reveals distinct fragmentation patterns. In 2020, generally, the NP was relatively stable, only dropping down within the 800–1000 m zone for the lowest and starting to increase until 2000 m. The highest values occurred between the 200 m and 800 m buffers, indicating a high degree of fragmentation in this zone at more than 70% (see Figure 7a). This contrasts with 1990, when the highest NP was found in the buffer under 200 m and decreased with distance from the river and the percentage of the NP in all of the buffer zone was still under 50% (see Figure 7b).

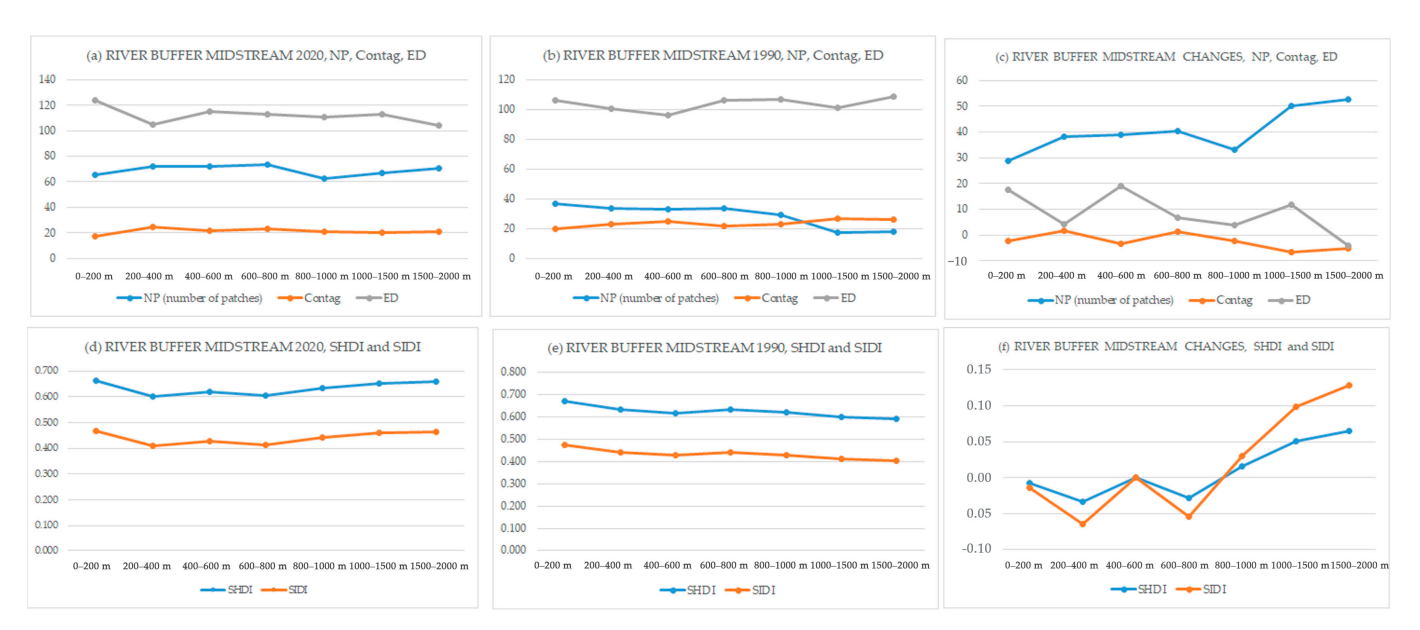


Figure 7. Midstream river buffer graphs.

When tracking the changes from 1990 to 2020, the most significant increases in NP occurred in the 1000 m to 2000 m buffers at around 50%, while the lowest changes were observed in the area under 200 m, suggesting relatively stable remaining green areas near the river (see Figure 7c).

The ED in 2020 was highest under 200 m before decreasing with distance. The contagion index remained relatively consistent over time across all buffers in 2020 and slightly increased in 1990 (see Figure 7a,b), with a notable exception of a high change within the 200–400 m buffer, with a positive value meaning increasing contagion (see Figure 7c).

The combination of a low NP but high ED and low Contag in the area closest to the river suggests a unique landscape fragmentation pattern of a few large, complexly shaped, yet disconnected patches, highlighting a distinct fragmentation dynamic that differs from the broader changes occurring further from the river.

Based on the analysis of the SHDI and SIDI indices in the midstream section of the Ciliwung River, the diversity patterns have shifted over 30 years. In 1990, diversity was highest closest to the river and decreased with distance. Conversely, in 2020, while the

highest diversity was still found in the buffer under 200 m, the overall trend was for diversity to increase with distance. However, the highest diversity is under 200 m in both years at around SHDI = 0.66 and SIDI = 0.47 (see Figure 7d,e). The table for the river buffer changes within the midstream area can be seen in Appendix A, Table A2.

Over the 30-year period, the changes in diversity were most significant further from the river (Figure 7f) with the diversity indices showing a positive value increase, meaning more diversity, starting from the 800 m buffer and increasing to their highest positive changes in the 1000–2000 m buffers. This indicates that the greatest increase in landscape diversity over the study period occurred in the outer zones of the midstream river buffer.

Downstream River Buffer

The NP in the Ciliwung River's downstream buffer shows different trends between 1990 and 2020. In 2020, the NP remained relatively stable, though it was slightly lower in the 600–800 m and 1500–2000 m buffer zones (Figure 8a). Conversely, in 1990, the NP generally increased as the distance from the river grew (Figure 8b). The most significant change in NP, with a roughly 50% increase, was observed in the area closest to the river (under 200 m buffer) (Figure 8c). This suggests that development has occurred primarily near the river within the time period. The lowest NP in 1990 was near the river, but in 2020, the NP was stable across all buffer zones. This, combined with the highest NP change occurring under 200 m, reinforces the conclusion that development has been most significant in the immediate vicinity of the river (Figure 8c).

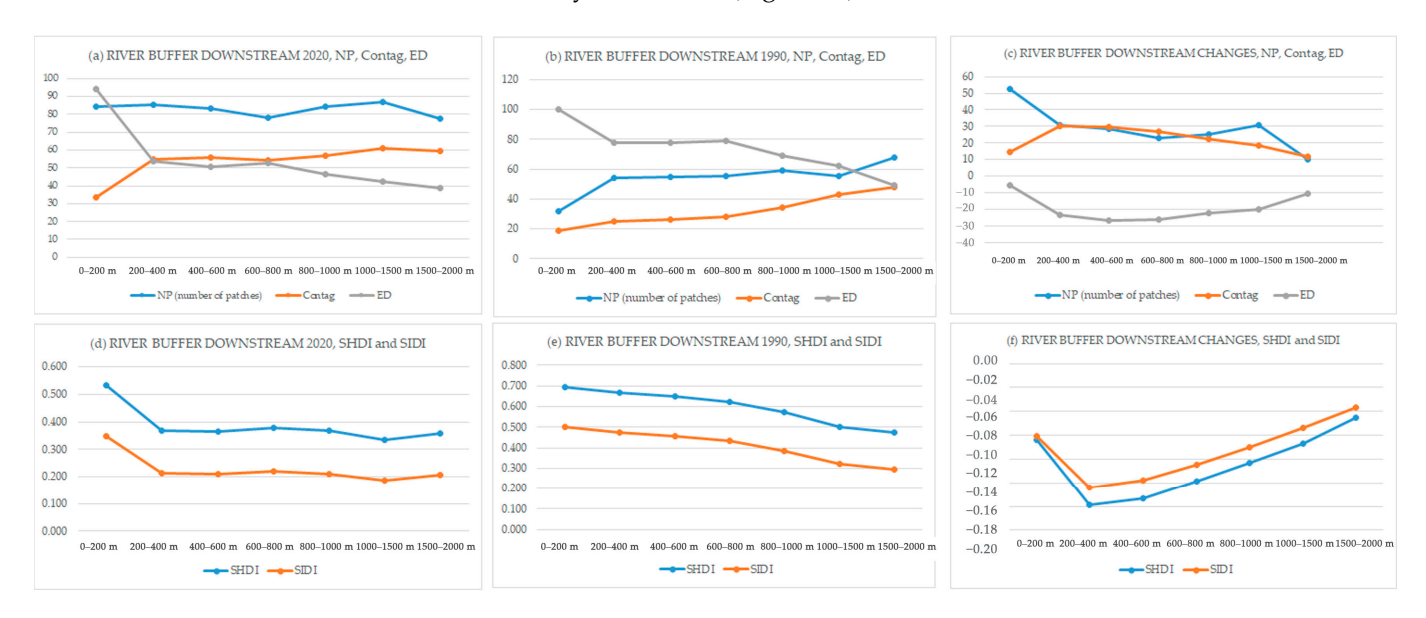


Figure 8. Downstream river buffer graphs.

As expected, the ED and Contag metrics exhibit an inverse relationship. For both 1990 and 2020, ED values were lower further away from the river, while Contag values were higher. The changes in these metrics also show an opposite trend (Figure 8a,b). The highest change in contagion occurred in the 200–600 m buffer areas, with a positive value, increasing aggregation, indicating a significant change in connectivity. Meanwhile, the lowest change in ED was within the 400–600 m buffer zone, with a negative value, meaning a decrease in patches or less fragmentation. This suggests that improvements, or at least a high change in connectivity, occurred in the 200–600 m areas (Figure 8c). River buffer changes within the downstream area are shown in Appendix A, Table A3.

Land 2025, 14, 2127 14 of 29

The diversity indices, including Shannon's diversity index (SHDI) and Simpson's diversity index (SIDI), were highest in the area closest to the river (under 200 m) in both 1990 and 2020 (Figure 8d,e). The changes in diversity were also most pronounced in the area under 200 m, decreased in the 200–400 m range, and then started to increase again further from the river. The negative values indicate that overall diversity decreased from 1990 to 2020. Although diversity changes increase with distance from the river, this overall decline persisted (Figure 8f).

Across the three river segments, the midstream Ciliwung watershed area exhibits a unique landscape fragmentation phenomenon. The NP is low close to the river, but high in ED and low in Contag. This suggests the area has complexly shaped, fragmented, few, large, but unconnected patches and showcases a pattern that differs from the fragmentation dynamics further from the river.

In the upstream area, the NP was high in the 0 to 600 m river buffer in both 1990 and 2020, with the greatest change occurring within the 200–400 m zone. The high ED in this area indicates low connectivity. Additionally, the diversity index showed a decline in the 200–400 m buffer in 1990, and a more consistent decrease with distance from the river in 2020.

However, in the downstream area, the area nearest to the river under a 200 m buffer experienced the most significant change in NP over the past 30 years. In both 1990 and 2020, this area showed low connectivity and a high degree of patchiness, evidenced by a low Contag and a high ED. Furthermore, all diversity indices across all buffer zones showed negative values, indicating an overall decrease in diversity from 1990 to 2020.

Upstream Road Buffer

Based on Figure 9a,b, the NP in the upstream Ciliwung River/watershed, as a measure of fragmentation, shows a general decrease as the distance from the road increases for both the 1990 and 2020 timeframes. The area closest to the road (under 200 m) is the most fragmented, with the highest % NP in both years (49% in 2020 and 31% in 1990). The change in NP between 1990 and 2020 is most significant near the road, showing a large increase of 17% within the "under 200 m" zone (see Figure 9c). This trend gradually diminishes with distance, eventually becoming a negative change at the 1000 m–1500 m and 1500 m–2000 m buffer zones, indicating a decrease in fragmentation in those areas over time. Contag, which signifies greater connectivity, generally increases with distance from the road for both 1990 and 2020, with the lowest values consistently found in the "under 200 m" buffer zone (Figure 9c).

ED, which indicates higher patchiness, shows the opposite trend, with values generally decreasing as the distance from the road increases for both timeframes. This suggests that the area closest to the road is the most fragmented and least connected, as evidenced by a high ED (Figure 9a,b). The changes in ED between 1990 and 2020 fluctuate across the buffer zones, while the changes in Contag generally increase with distance, showing a significant increase of 14 units at the furthest buffer zone (see Figure 9c).

SHDI and SIDI consistently decrease with increasing distance from the road in both 1990 and 2020 (Figure 9d,e). The highest diversity values for both timeframes are found in the "under 200 m" zone, dropping off significantly in the more distant buffer zones. The graphs show that the decrease in diversity is steeper for the 2020 data compared to the 1990 data, particularly in the 1500 m–2000 m range. The changes in both SHDI and SIDI between 1990 and 2020 are predominantly negative, indicating a decrease in diversity over time, with the most significant drop occurring beyond the 800 m buffer zone (see Figure 9f). The table for the road buffer changes within the upstream area can be seen in Appendix A, Table A4.

Land 2025, 14, 2127 15 of 29

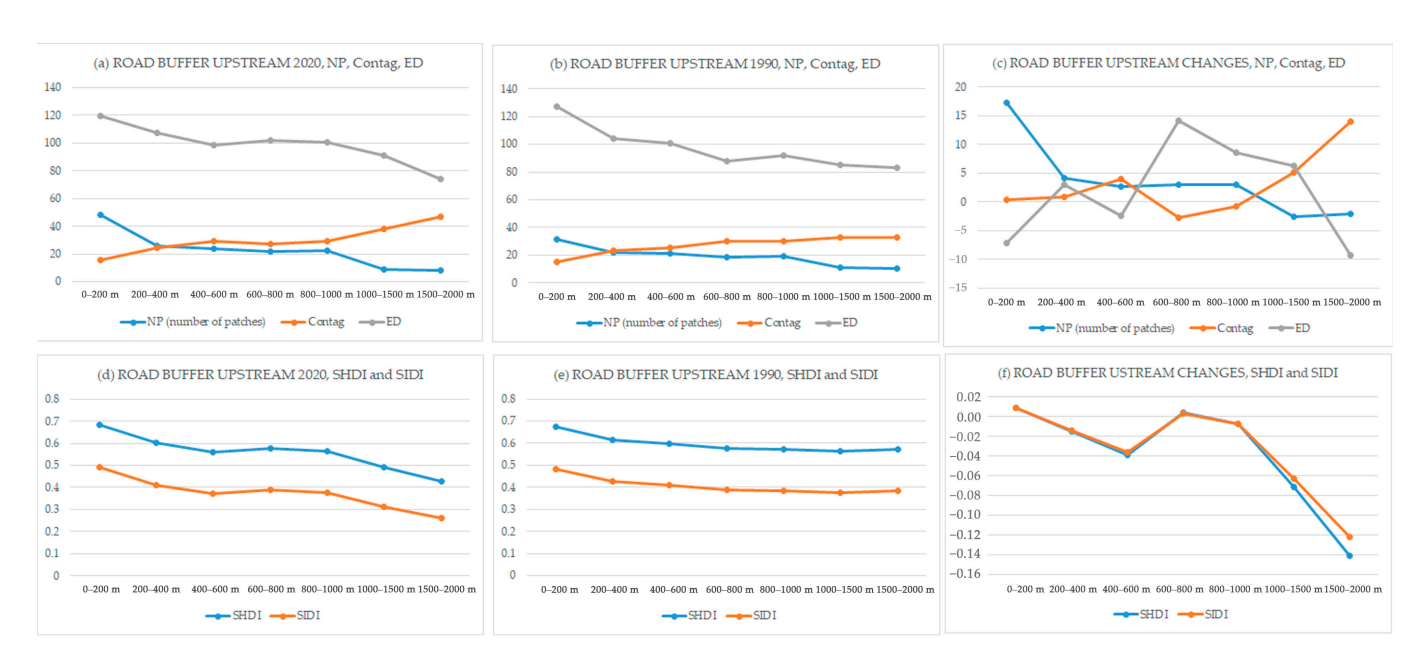


Figure 9. Upstream road buffer graphs.

Midstream Road Buffer

In 1990, the NP was highest near the road, within the under 200 m buffer, and decreased gradually with distance up to 1500–2000 m (Figure 10b). However, the 2020 data presents a slightly different pattern, with the highest NP values observed near the road and again at the 1500–2000 m distance, creating a shallow U-shape on the graph (Figure 10a). The change in NP between 1990 and 2020 was highest at the 1500–2000 m distance, with a difference of 60% (Figure 10c).

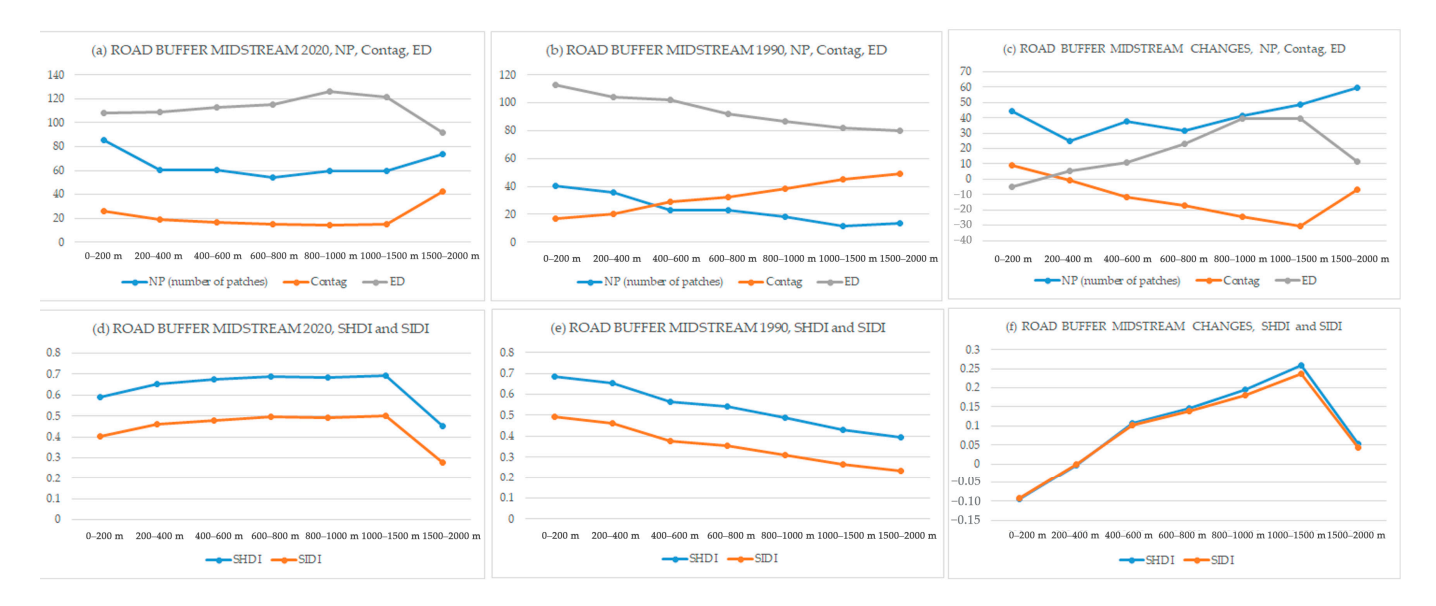


Figure 10. Midstream road buffer graphs.

The Contag in 1990 showed a pattern opposite to that of the NP, increasing with distance from the main road (Figure 10b). In 2020, the Contag index followed a similar U-shaped pattern to the NP, with the highest values observed at the 1500–2000 m distance (Figure 10a). The greatest negative change in the Contag index, indicating an increase in patchiness, occurred in the 1000–1500 m buffer with a decrease of 30 points between 1990 and 2020 (Figure 10c).

Land 2025, 14, 2127 16 of 29

In 1990, the ED had a pattern similar to the NP, decreasing from the 200 m buffer toward the 2000 m buffer (Figure 10b). The pattern in 2020 was the opposite, with ED increasing until it peaked at the 800–1000 m buffer before declining toward 2000 m (Figure 10a). The change in ED between 1990 and 2020 increased steadily from the road until reaching its peak difference within the 800–1000 and 1000–1500 m buffers, with a difference of 39 points in both areas (Figure 10c). This significant change suggests that these areas became more fragmented and patchier over the 30-year period.

In 1990, SHDI and SIDI were highest near the road, in the under 200 m buffer, and gradually declined with distance up to 2000 m (Figure 10e). The 2020 data shows a different trend, with both diversity indices starting low, increasing to a peak at the 1000–1500 m buffer, and then dropping sharply at the 1500–2000 m buffer (Figure 10d). The changes in both SHDI and SIDI between 1990 and 2020 were most significant in the 1000–1500 m buffer, with positive changes of 0.26 and 0.24, respectively, indicating that diversity increased in this area over the period (Figure 10f). At the 1500–2000 m buffer, however, the changes in the NP were high, which indicates greater fragmentation. Despite this, the diversity indices remained lower, showing only a slight increase in diversity compared to the peak observed at 1000–1500 m. Road buffer changes within the midstream area are shown in Appendix A, Table A5.

Downstream Road Buffer

Based on Figure 11a,b, in 1990, the NP for the downstream road buffer of the Ciliwung River generally decreased from under 200 m to 2000 m. In contrast, the NP in 2020 showed a different trend, initially decreasing and then increasing, with a slight drop between 1000 and 1500 m before increasing again toward 2000 m.

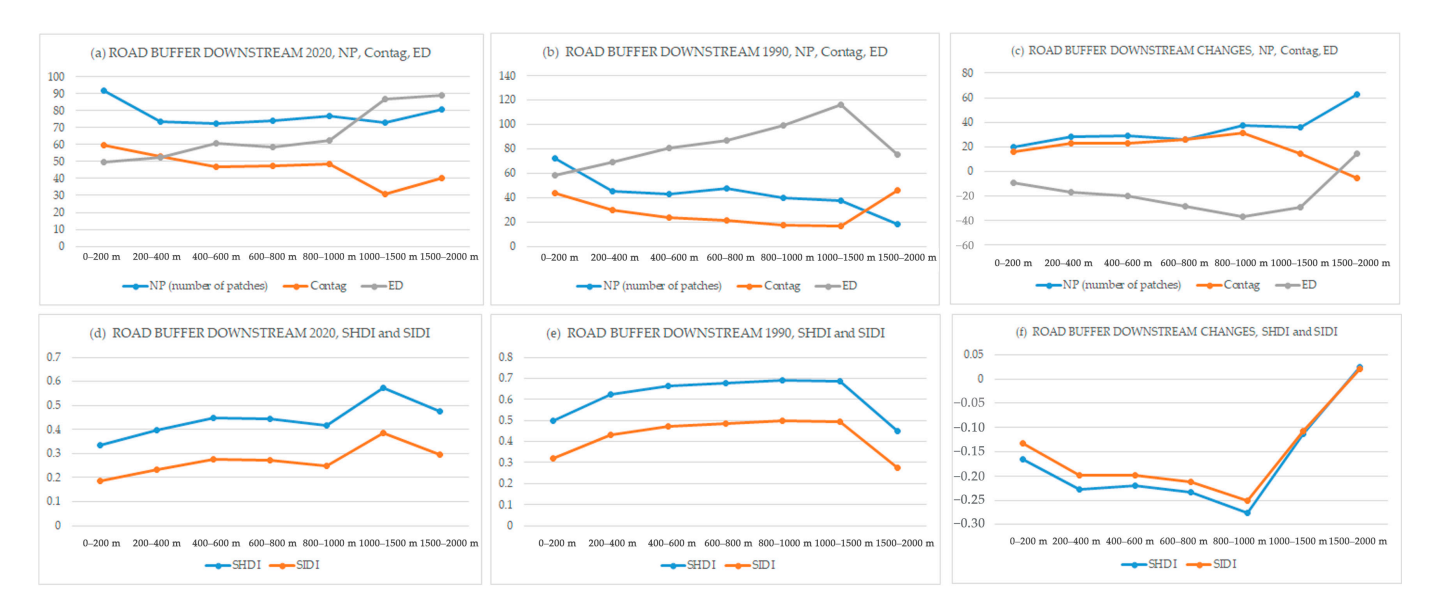


Figure 11. Downstream road buffer graphs.

The change in NP from 1990 to 2020 was a general increase across all buffer zones, with the highest increase observed in the 1500–2000 m zone (Figure 11c). This suggests that the area became more fragmented or "patchy" over the 30-year period, particularly at a greater distance from the main road.

The contagion index (Contag) in 1990 followed a similar pattern to NP, decreasing from under 200 m to 1500 m. However, unlike NP, it then increased dramatically within the 1500–2000 m buffer. In 2020, the contagion index, however, generally followed the same pattern as NP (Figure 11a,b). The highest increase in the contagion index from 1990 to 2020

Land 2025, 14, 2127 17 of 29

was observed in the 800–1000 m buffer with 31 unit changes. This indicates an increase in connectivity within this area (Figure 11c).

The ED showed an opposite pattern to the contagion index in both 1990 and 2020. In 1990, the ED was highest in the 1000–1500 m buffer zone, while in 2020, the highest ED value was in the 1500–2000 m zone (Figure 11a,b). A higher ED indicates a more fragmented and patchy landscape. The changes in ED from 1990 to 2020 show a negative trend in most buffer zones, indicating a decrease in ED from 1990 to 2020. This suggests the area became less fragmented, with the exception of the 1500–2000 m zone, which saw a significant increase (Figure 11c).

The diversity indices, including SHDI and SIDI, both showed almost a similar trend in 1990 and 2020 (Figure 11d,e). In 1990, both indices generally increased gradually from under 200 m to 1500 m and then dropped. The 2020 data followed a similar pattern, although a slight decrease was observed within the 600–1000 m range.

The changes in diversity indices from 1990 to 2020 showed a significant increase in the 1000–2000 m range (Figure 11f). This indicates a greater difference in diversity between the two periods. The positive values suggest an increase in diversity, which stands in contrast to other buffers that showed a decrease in diversity over the 30-year period, specifically in the 200 m to 1000 m buffers.

Based on the analysis of these landscape metrics, it appears that significant development or land-use change occurred in the downstream Ciliwung River road buffer. The NP was initially highest near the road in 1990, but by 2020, the NP had increased across all buffer zones, with the highest NP still located close to the main road (see Figure 11a,b).

The data also indicates that the highest level of fragmentation and landscape change took place in the buffer zones starting from 800 m away from the roads, with the most pronounced changes occurring in the 1500–2000 m zone (see Figure 11c). The trends of high changes in NP and ED, combined with high diversity indices and low Contag, all point to increased patchiness and less connectivity in the outer buffer zones over the 30-year period.

The table for the road buffer changes within the downstream area can be seen in Appendix A, Table A6.

Across the upstream, midstream, and downstream segments, the highest NP in both 1990 and 2020 consistently occurred in the buffer zone closest to the main road (under 200 m buffer zone), indicating that these areas were the most fragmented. In the upstream segment, this fragmentation near the road correlates with high ED, high diversity, and low Contag.

In the midstream and downstream segments, however, the most significant changes in fragmentation between 1990 and 2020 occurred within the 1500–2000 m buffer zone, which is furthest from the main road.

For the midstream segment, the increase in fragmentation is supported by a large positive change in NP, particularly in the 1500–2000 m buffer zone where the change was highest. The ED also showed significant positive changes within the 800–1500 m buffers, peaking at a 39-point increase, which indicates increased patchiness and fragmentation in these areas. However, the change in ED drops significantly in the 1500–2000 m buffer. When combined with the high NP change, this suggests that while the landscape became more fragmented and scattered into individual patches, the overall shape complexity of those patches decreased. This outcome aligns with findings on the effects of negative fragmentation [45,46].

Additionally, despite the fragmentation, there was a notable increase in diversity in the 1000–1500 m buffer, suggesting a more complex pattern of land-use change. This indicates that new types of land cover were introduced, even as the overall landscape became more fragmented and isolated.

Land 2025, 14, 2127 18 of 29

In the downstream segment, the highest increase in fragmentation, as measured by a large positive change in NP, occurred in the 1500–2000 m buffer zone. This is further supported by a significant increase in ED in this same zone, indicating the creation of more patches with complex edges.

However, the data reveals a more nuanced picture. Contrary to a simple fragmentation narrative, there was a significant increase in connectivity (positive value change in contagion) in the 800–1000 m zone. This indicates that some parts of the landscape became more connected over the period.

Furthermore, the diversity indices (SHDI and SIDI) showed a general decrease from 1990 to 2020 within the 200–1500 m buffers. This trend then reverses, with a significant increase in diversity in the 1500–2000 m buffer, which stands in contrast to the trends observed in the midstream and upstream segments. This suggests that while fragmentation increased, it also led to a more diverse landscape in the areas furthest from the main road.

To sum up, while the area near the main road is consistently the most fragmented across all three segments, the most significant changes in fragmentation from 1990 to 2020 took place further from the road in the midstream and downstream areas. This fragmentation condition impacts LULC change. Specifically, the built-up area, including settlements, expanded within the study timeframe in both the midstream and downstream areas, heavily occurring far from the main road networks. In contrast, the upstream zone's LULC change is characterised by ribbon infrastructure, with built-up areas predominantly dominating the land directly along the main road. These changes are not uniform and show complex interactions, such as increased fragmentation alongside increased diversity and, in some cases, increased connectivity.

3.2. Discussion

3.2.1. Relationship Between River and Road Buffer Fragmentation

Fragmentation patterns based on NDVI changes, measured by green loss, show distinct trends between river and road buffers across the three segments of the Ciliwung River. For river buffers, fragmentation is generally most severe close to the river in the upstream and downstream segments, where green loss is high near the river and decreases with distance. However, the midstream segment is unique: while it experiences significant fragmentation, green areas remain close to the river, with the highest green loss occurring further out in the 400–600 m buffer.

In contrast, road buffer fragmentation shows a different pattern. Upstream, changes are most pronounced near the main road. However, in the midstream and downstream, the most significant fragmentation occurs far from the main road, specifically in the 1000–2000 m buffers.

The upstream segment faces a specific challenge where high green loss occurs near both the river and road (0–400 m). Although the aggregate NDVI change for vegetation loss is not as high as in the midstream, it is noted that the area is close to a prominent protected area, the Gunung Gede Pangrango National Park, which requires further monitoring.

Generally, the NP was high in 2020 across all segments near both the river and the main road, with values accumulating in the 0–600 m buffer zone. However, the nature of fragmentation changes is unique and distinct, particularly in the midstream. Here, the landscape is highly fragmented into many small, unconnected patches with low shape complexity, a pattern that sets it apart from other areas. Additionally, significant changes in landscape fragmentation occur in the midstream and downstream segments far from the main road (specifically, within the 1500–2000 m buffer). This suggests that the development of secondary, tertiary, and informal roads is a primary cause of fragmentation away from the main thoroughfares in the midstream and downstream sections. In the upstream sections,

Land 2025, 14, 2127 19 of 29

however, fragmentation is primarily caused by the main roads. These unique and dynamic trends highlight how different LULC changes drive unique fragmentation processes.

The findings underscore that road-induced fragmentation extends beyond primary road infrastructure. Given that Mohammadi and Fatemizadeh [23] found significant degradation within a 1000 m highway buffer, future research should explore whether lower-class roads (such as tertiary or local and informal roads, which are increasingly dense in the Ciliwung watershed) exert a comparable fragmenting force, as their cumulative impact may be substantial. For river fragmentation, this research analysis shows a unique midstream fragmentation character, confirming that the closest buffer to the mainstream remains intact but is the most ecologically sensitive area. This aligns with research by Yirigui et al. [24], who emphasised that fragmentation near the streamline disproportionately impacts ecological communities (diatoms, macroinvertebrates, and fish).

Furthermore, Deere et al. [47] found that a "one-size-fits-all" buffer policy is inadequate when examining riparian buffers in Southeast Asian oil palm agriculture. While narrower buffers (e.g., 30–40 m) could be sufficient for maintaining overall richness for many faunal taxa, wider buffers (e.g., 100–200 m) are necessary to facilitate species movement and maintain ecological connectivity, especially for sensitive, forest-dependent species. Consequently, buffer width recommendations should be context-dependent and require the definition of target taxa (considering both terrestrial and aquatic communities).

This is crucial, as the landscape riverine characteristics of this research vary considerably—the downstream area is urbanised, the upstream is more rural, and the transitional or midstream area has mixed environments, all of which require considering different species or taxa targets. Therefore, planning and management efforts must prioritise the protection and restoration of the immediate riparian strip closer to the mainstream and both narrow and broader river buffer widths should be carefully considered to maintain ecological function. It is essential to recognise that both road and river features possess distinct characteristics. Policy designation should, thus, be informed by these two linear features as key landscape components when addressing their impact on LULC.

The case study of the transition zone of Bogor City and Regency, located in the midstream Ciliwung River watershed, faces many challenges due to population increases. This research confirms settlement expansion in this area—encompassing both urban and rural sprawl and characterised by uneven development. This has the potential to exacerbate habitat isolation, thereby accelerating ecological degradation [22,25,48].

3.2.2. Landscape Fragmentation Dynamics Divergence Along the Ciliwung Riverine Gradient

The landscape metrics reveal a fundamental divergence in the process of urban impact across the Ciliwung River watershed, which is critical for policy designation. In the upstream and midstream areas, the landscape change is predominantly characterised by fragmentation. This region functions as the active urban–rural fringe, where the abundant vegetation land available in 1990, primarily forest, plantation, and agriculture, is being actively consumed by dispersed, low-density development. NDVI classification change confirms areas of high non-vegetated built-up classes suggesting that large natural habitats are being broken up, perforated, and divided in the midstream. In contrast, changes upstream show evidence of greening (forest shifting to plantation and agricultural land). This process is exacerbated by linear infrastructure, such as ribbon development along roads particularly in the upstream area, and the riverbanks themselves in the midstream which isolate remaining patches. This outcome aligns with the findings of Marwasta [49], who found that concentric and dispersed urban growth patterns, including compact fan shape and leapfrogging development, dominate the expansion of the Jakarta area into its hinterland.

Land 2025, 14, 2127 20 of 29

In sharp contrast, the downstream area of the Ciliwung River, which encompasses the core of Jakarta, exhibits a pattern dominated by densification and complete loss, rather than fragmentation. By 1990, the natural land cover in this area was already scarce and notably isolated starting near the main roads, and much of the natural area near the river was already beginning to be lost. This finding corroborates the research of Fachrul et al. [50], which states that settlement developed in the riverbanks starting in 1980 and spread widely to Bogor Regency during 1990 to 2000. According to Pribadi and Pauleit [51], urban expansion in the Jakarta metropolitan area began in the early 1980s with the development of toll roads in an east—west direction, aiming to control growth toward the south, an important water supply area. Therefore, the landscape dynamic over the last three decades has focused on the consolidation of the built-up matrix. This is reflected in a non-vegetated or high built-up class, indicating the remaining agricultural plots have been consumed to create a larger, more cohesive urban area. Pribadi and Pauleit [51] explained that the urban expansion of Jakarta between 1995 and 2005 developed in all directions and resulted in the replacement of agricultural areas.

For the few remaining green space patches, the gradually declining NP changes in the river buffer (far from the main river) and the almost stable NP in 2020 across the river and road buffer signify loss and less breaking apart. This distinction is important, as while the upstream and midstream face an ecological crisis defined by forest loss and changes, the downstream area is characterised by a high urban area, low stable green area, and very low levels of greening (based on NDVI classification changes). Consequently, the downstream area faces a socioeconomic–environmental crisis defined by the critical scarcity of green–blue infrastructure and the resultant loss of essential ecosystem services, such as flood and climate mitigation. This finding supports the research of Sumarga et al. [52] and Kurniawan et al. [53], who identified that Jakarta faces key environmental problems, such as flooding and climate change, which result in damage extending beyond physical harm to include socioeconomic issues, including population, land-use policies, and road development stemming from urbanisation and expansion.

3.2.3. Future Environmental, Ecological, and Natural Resource Preservation and Limitations

Based on the research findings on landscape fragmentation changes, future preservation efforts in urban–rural riverine contexts should adopt a targeted, strategic approach, moving beyond generalised institutional frameworks. The research reveals that fragmentation is not uniform but follows dynamic patterns driven by specific land-use/land-cover (LULC) changes and road infrastructure types. A deeper integration of existing ecological theory and empirical studies can provide a more robust foundation for these strategic recommendations.

The observed patterns of fragmentation align with concepts such as patch–corridor—matrix models and the intermediate disturbance hypothesis, which posits that a moderate level of disturbance can increase biodiversity by creating a mosaic of habitats [54,55]. The study's findings on river buffers, where fragmentation is high upstream and downstream while green areas persist immediately adjacent to the midstream, suggest that the midstream as a transitional area could act as a critical riparian corridor that needs to be preserved to maintain biodiversity and ecosystem services. This confirms the importance of riparian zones as essential ecological corridors for gene flow and species movement, as extensively documented in the fluvial geomorphology and landscape ecology literature [56]. Restoring these corridors, particularly in highly fragmented upstream and downstream segments, is a priority for maintaining biodiversity and ecosystem services [57].

Fragmentation near roads is most severe further from main roads in the midstream and downstream, driven by secondary, tertiary, and or informal road development. This

highlights the need for proactive future land-use planning and design in an urban riparian environment [58]. Instead of broad policies and institutionalisation, preservation efforts must focus on controlling the spread of micro-road infrastructure that creates fragmented, isolated patches. The findings on micro-road development resonate with the concept of edge effects, where the presence of roads and other linear infrastructure creates distinct habitat boundaries, increasing stress on interior species and facilitating the spread of invasive species, a phenomenon well-documented in conservation biology [59,60].

By understanding these distinct drivers, cities can implement effective, locationspecific strategies to manage development, preserve critical habitats, secure natural resources against urban expansion, and create ecological connectivity within the buffer area of both river and road infrastructure.

It is important to acknowledge the limitations of the methodological approach. The use of a cut-off threshold for NDVI to delineate vegetated areas, rather than a continuous analysis, simplifies a complex ecological reality. This binary classification can oversimplify spatial patterns, potentially misrepresenting areas of low-density vegetation or transition zones that still hold ecological value. Future studies could employ a continuous approach to better characterise the spatial heterogeneity of the landscape and provide a more finegrained assessment of fragmentation impacts [61]. The 30 m pixel size can lead to the omission of smaller, linear features, such as narrow riparian buffers or newly constructed informal pathways. This potentially underestimates the true extent of fine-scale fragmentation and edge effects, particularly at the highly complex, heterogeneous urban–rural interface. Although a higher resolution could increase the NP, leading to different interpretations and understanding, this study also suggests that future research could more thoroughly and carefully explore how remote-sensing and GIS technologies can be used.

Another limitation is the focus on structural fragmentation (physical breaks in the land-scape) without fully analysing functional fragmentation (the ecological and behavioural impacts on species movement) [62]. While road density is a key driver, the specific design of these roads such as culvert locations or the presence of wildlife crossings and their impact on animal movement was not assessed. These are critical aspects of connectivity that go beyond simple spatial metrics.

Given these insights, future preservation efforts must focus on controlling the spread of micro-road infrastructure and managing the rapid LULC changes that create fragmented, isolated patches. This requires a shift from broad, reactive policies to proactive, location-specific planning [63,64]. Further study should explore the transitional areas as a more dynamic urban–nature landscape pattern. Cities can implement effective, location-specific strategies to manage development, preserve critical habitats, and secure natural resources against urban expansion by understanding these distinct drivers. This could involve incorporating ecological connectivity models into urban planning and policy, focusing on the preservation and restoration of key ecological corridors [65].

4. Conclusions

This study investigated how urban and rural development affects landscape fragmentation along the Ciliwung River, Indonesia, by analysing changes in land-use/land-cover (LULC) between 1990 and 2020 using remote-sensing and GIS technologies. The research aimed to deepen the understanding of how river and road infrastructure networks influence fragmentation in a highly populated megacity context via catchment-scale analysis.

The findings reveal distinct fragmentation patterns across the river's three segments: upstream, midstream (transition), and downstream. The most significant fragmentation, measured by green space loss, occurred in the midstream or transitional area of the watershed. This area, which constitutes part of the urban periphery of Jakarta, is experiencing

Land 2025, 14, 2127 22 of 29

accelerated and severe fragmentation and habitat loss. This pattern highlights a detrimental trend of rapid, high-density urban growth (doughnut), which particularly impacts species migration across urban–rural corridors.

River buffer analysis showed that in the upstream and downstream segments, fragmentation was most severe near the river. In contrast, the midstream area is unique; it had significant fragmentation overall, with the highest green loss occurring further out in the 400–600 m buffer. This segment is characterised by metrics that suggest a distinct fragmentation change dynamic, with low NP, high ED, and low Contag values particularly observed in the area closest to the river.

Fragmentation patterns near main roads exhibited a different trend. While fragmentation was most pronounced near the road in the upstream segment, the midstream and downstream areas experienced the most significant changes far from the main road, specifically over 1000 m away. This suggests that the expansion of secondary and informal roads is a primary driver of fragmentation in these sections. Overall, the study highlights how different landscape features, specifically rivers and road infrastructure, drive unique fragmentation processes within the megacity. It underscores the integral role of remote sensing and GIS in monitoring LULC change and informing future environmental, ecological, and natural resource preservation efforts.

A key lesson from this research is the critical need for LULC analysis to incorporate the distinct landscape fragmentation effects of both riverine and road infrastructure. This study found that these two features create significantly different fragmentation patterns, impacting natural resources and urban ecosystems in unique ways. Therefore, a comprehensive and multifaceted approach to urban planning, design, and conservation must move beyond a generalised view of LULC change and consider these specific drivers of fragmentation. This study empowers urban planners, designers, and policymakers to develop more careful, sustainable solutions for managing the complex interplay between human development and the preservation of natural landscapes in highly populated areas and demonstrates the power of integrating GIS and remote-sensing technologies.

Author Contributions: Conceptualization, P.B., R.K., N.D. and T.W.; methodology, P.B. and R.K.; software, R.K.; validation, R.K.; formal analysis, R.K.; data curation, R.K.; writing—original draft preparation, R.K.; writing—review and editing, P.B., R.K., N.D. and T.W.; visualization, R.K.; supervision, P.B.; project administration, R.K.; funding acquisition, R.K. All authors have read and agreed to the published version of the manuscript.

Funding: This paper is derived from doctoral research of the first author, which is funded and supported by the Indonesia Endowment Fund for Education Agency (LPDP).

Data Availability Statement: This study utilised open-source Landsat 5 and 8 satellite imagery, sourced from the USGS (https://earthexplorer.usgs.gov (accessed on 20 March 2022)). The vector road data used for buffering were obtained through personal communication from the Public Works and Spatial Planning Agency, City of Bogor (https://dpupr.kotabogor.go.id/home (accessed on 20 March 2022)). The vector river data used for buffering was obtained through personal communication from the Ciliwung-Cisadane River Region Authority (BBWS), the Ministry of Public Works and Housing (PUPR), Directorate General of Water Resources (https://sda.pu.go.id/balai/bbwscilicis (accessed on 20 March 2022)).

Conflicts of Interest: The authors declare no conflicts of interest.

Land **2025**, 14, 2127 23 of 29

Abbreviations

The following abbreviations are used in this manuscript:

NDVI	Normalised Difference Vegetation Index	SHDI	Shannon's Diversity Index
LULC	Land Use/Land Cover	SIDI	Simpson's Diversity Index
GIS	Geographic Information Systems	Contag	Contagion
NP	Number of Patches	ED	Edge Density

Appendix A

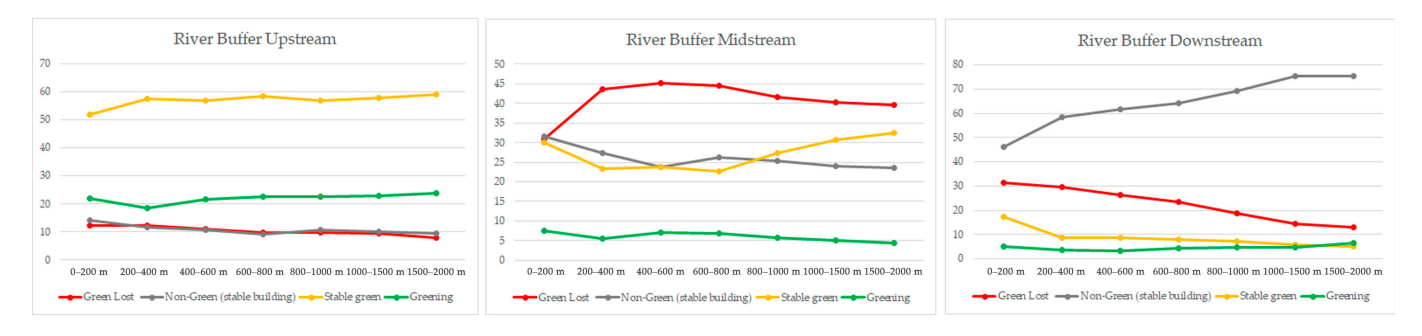


Figure A1. River buffer graphs, % of fragmentation changes from 1990 to 2020.

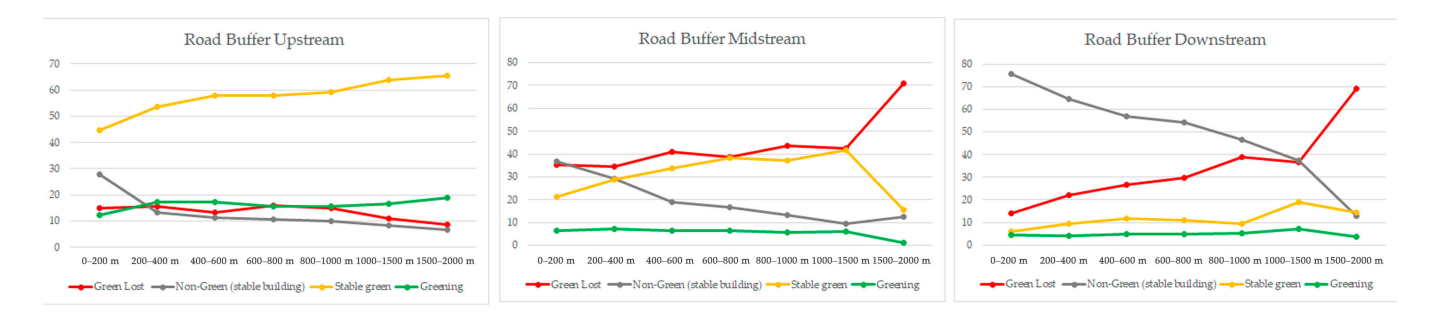


Figure A2. Road buffer graphs, % of fragmentation changes from 1990 to 2020.

Table A1. Upstream river buffer changes.

		0–200 m	200–400 m	400–600 m	600–800 m	800–1000 m	1000–1500 m	1500–2000 m
2020								
	NP (number of patches)	24	25	24	20	22	12	10
	SHDI	0.576	0.551	0.523	0.488	0.511	0.492	0.460
	SIDI	0.388	0.364	0.340	0.309	0.329	0.313	0.286
	Contag	29.293	32.723	36.052	39.536	38.027	40.103	45.726
	ED	96.939	86.158	81.382	79.724	76.092	78.185	64.290
1990								
	NP (number of patches)	22	21	24	23	21	17	13
	SHDI	0.652	0.612	0.629	0.626	0.636	0.634	0.635
	SIDI	0.460	0.421	0.437	0.434	0.444	0.442	0.443
	Contag	21.260	27.883	25.667	27.296	26.591	28.999	31.148
	ED	104.298	83.509	86.549	80.587	79.779	73.923	64.318
Changes								
O	NP (number of patches)	1	4	1	-3	1	-5	-3
	SHDI	-0.07623	-0.06124	-0.10579	-0.13806	-0.12552	-0.14138	-0.17488
	SIDI	-0.07215	-0.05656	-0.09730	-0.12509	-0.11520	-0.12870	-0.15723
	Contag	8	5	10	12	11	11	15
	ED	-7	3	-5	-1	-4	4	0

Land **2025**, 14, 2127 24 of 29

 Table A2. Midstream river buffer changes.

		0–200 m	200–400 m	400–600 m	600–800 m	800–1000 m	1000–1500 m	1500–2000 m
2020								
	NP (number of patches)	66	72	72	74	63	67	70
	SHDI	0.662	0.601	0.619	0.606	0.635	0.651	0.658
	SIDI	0.469	0.411	0.427	0.415	0.443	0.459	0.465
	Contag	17.210	24.558	21.409	22.937	20.640	19.919	21.054
	ED	123.568	104.621	114.818	112.702	110.768	112.887	104.163
1990								
	NP (number of patches)	37	34	33	33	29	17	18
	SHDI	0.669	0.634	0.619	0.633	0.619	0.601	0.592
	SIDI	0.476	0.442	0.427	0.441	0.428	0.411	0.402
	Contag	19.686	22.756	24.938	21.801	22.849	26.518	26.248
	ED	105.927	100.516	95.794	105.954	106.828	100.985	108.362
Changes								
	NP (number of patches)	29	38	39	40	33	50	52
	SHDI	-0.00727	-0.03290	0.00008	-0.02771	0.01555	0.05009	0.06546
	SIDI	-0.00714	-0.03122	0.00007	-0.02633	0.01485	0.04783	0.06243
	Contag	-2	2	-4	1	-2	-7	-5
	ED	18	4	19	7	4	12	-4

Table A3. Downstream river buffer changes.

		0–200 m	200–400 m	400–600 m	600–800 m	800–1000 m	1000–1500 m	1500–2000 m
2020								
	NP (number of patches)	84	85	83	78	84	87	78
	SHDI	0.533	0.368	0.364	0.378	0.367	0.334	0.359
	SIDI	0.349	0.212	0.209	0.219	0.211	0.187	0.205
	Contag	33.372	54.998	55.852	54.377	56.871	61.106	59.587
	ED	94.274	53.953	50.699	52.529	46.697	42.115	38.529
1990								
	NP (number of patches)	32	54	55	55	59	56	68
	SHDI	0.693	0.665	0.647	0.624	0.574	0.501	0.472
	SIDI	0.500	0.472	0.455	0.432	0.386	0.321	0.296
	Contag	18.782	24.737	26.022	27.806	34.296	42.722	47.868
	ED	100.085	77.529	77.779	78.889	69.218	62.070	49.163
Changes								
O	NP (number of patches)	52	31	28	23	25	31	10
	SHDI	-0.15998	-0.29759	-0.28266	-0.24606	-0.20714	-0.16733	-0.11364
	SIDI	-0.15122	-0.26058	-0.24533	-0.21274	-0.17450	-0.13430	-0.09105
	Contag	15	30	30	27	23	18	12
	ED	-6	-24	-27	-26	-23	-20	-11

Table A4. Upstream road buffer changes.

		0–200 m	200–400 m	400–600 m	600–800 m	800–1000 m	1000–1500 m	1500–2000 m
2020								
	NP (number of patches)	49	26	24	22	23	9	8
	SHDI SIDI Contag ED	0.683 0.490 15.852 119.792	0.602 0.412 24.309 107.149	0.561 0.373 29.551 98.642	0.579 0.390 27.366 102.009	0.563 0.375 29.008 100.310	0.491 0.312 38.001 91.103	0.429 0.260 46.607 73.830
1990	ED	119.792	107.149	96.042	102.009	100.510	91.103	73.630
	NP (number of patches)	31	22	21	19	20	11	10
	SHDI SIDI Contag ED	0.674 0.481 15.436 127.037	0.617 0.426 23.391 104.185	0.600 0.410 25.496 100.993	0.575 0.387 30.155 87.845	0.570 0.382 29.809 91.737	0.562 0.375 32.914 84.835	0.570 0.382 32.552 83.136
Changes	NP (number of patches)	17	4	3	3	3	-3	-2
	SHDI SIDI Contag ED	$0.00864 \\ 0.00856 \\ 0 \\ -7$	$ \begin{array}{r} -0.01468 \\ -0.01385 \\ \hline 1 \\ 3 \end{array} $	$-0.03928 \\ -0.03625 \\ 4 \\ -2$	$0.00383 \\ 0.00353 \\ -3 \\ 14$	$ \begin{array}{r} -0.00757 \\ -0.00691 \\ \hline -1 \\ 9 \end{array} $	$ \begin{array}{r} -0.07134 \\ -0.06309 \\ \hline 5 \\ \hline 6 \end{array} $	$ \begin{array}{r} -0.14158 \\ -0.12240 \\ \hline 14 \\ -9 \end{array} $

Land 2025, 14, 2127 25 of 29

0.10735

0.10201

-12 11

	0-200 m	200–400 m	400–600 m	600–800 m	800–1000 m	1000–1500 m	1500–2000 m
NP (number of patches)	85	61	60	54	60	60	73
SHDI	0.590	0.654	0.674	0.687	0.683	0.692	0.450
SIDI	0.401	0.461	0.481	0.494	0.490	0.499	0.277
Contag	26.384	19.266	16.826	15.107	13.879	14.868	42.350
ED	108.047	109.202	113.019	115.518	126.026	121.527	91.456
NP (number of patches)	41	36	23	23	18	12	14
SHDI	0.684	0.656	0.566	0.542	0.488	0.432	0.396
SIDI	0.491	0.463	0.379	0.356	0.309	0.263	0.234
Contag	17.030	20.113	28.689	32.392	38.367	45.015	49.206
ED	112.909	103.837	102.347	92.192	86.850	82.126	80.024

0.14570

0.13788

-17

23

0.19549

0.18100

-24 39

0.25968

0.23607

39

-30

0.05311

0.04287

11

Table A5. Midstream road buffer changes.

2020

1990

Changes

SHÒI

ED

Contag

NP (number of patches)

Table A6. Downstream road buffer changes.

-0.00229

-0.00223

-1 5

0.09432

-0.09076

9

-5

		0–200 m	200–400 m	400–600 m	600–800 m	800–1000 m	1000–1500 m	1500–2000 m
2020								
	NP (number of patches)	92	73	72	74	77	73	81
	SHDI	0.333	0.395	0.446	0.443	0.416	0.574	0.474
	SIDI	0.186	0.233	0.274	0.271	0.249	0.386	0.297
	Contag	59.720	52.989	46.731	47.661	48.842	31.037	40.404
	ED	49.688	52.186	60.829	58.582	62.472	86.756	89.249
1990								
	NP (number of patches)	72	45	43	48	40	37	18
	SHDI	0.499	0.624	0.666	0.677	0.693	0.687	0.448
	SIDI	0.319	0.432	0.473	0.484	0.499	0.494	0.276
	Contag	43.820	29.858	23.828	21.642	17.625	16.362	46.043
	ED	58.533	69.066	80.730	86.767	98.982	116.083	75.051
Changes								
O	NP (number of patches)	20	28	29	26	37	36	63
	SHDI	-0.16574	-0.22845	-0.21921	-0.23411	-0.27685	-0.11307	0.02534
	SIDI	-0.13280	-0.19907	-0.19837	-0.21244	-0.25004	-0.10826	0.02120
	Contag	16	23	23	26	31	15	-6
	ED	_9	-17	-20	-28	-37	-29	14

Appendix B

The formulas for the landscape metrics are as follows:

Appendix B.1. Number of Patches

Vector/Raster

NP = ni

Units: None.

Range: $NP \ge 1$, without limit.

NP = 1 when the landscape contains only 1 patch of the corresponding patch type, that is, when the class consists of a single patch.

Description: NP equals the number of patches of the corresponding patch type (class).

Appendix B.2. Shannon's Diversity Index

Vector/Raster

$$SHDI = -\sum_{i=1}^{m} (Pi o lnPi)$$

Units: None.

Range: SHDI \geq 0, without limit.

SHDI = 0 when the landscape contains only 1 patch (no diversity). SHDI increases as the number of different patch types (patch richness, PR) increases or the proportional distribution of area among patch types becomes more equitable, or both.

Land 2025, 14, 2127 26 of 29

Description: SHDI equals minus the sum, across all patch types, of the proportional abundance of each patch type multiplied by that proportion.

Appendix B.3. Simpson's Diversity Index

Vector/Raster

$$SIDI = 1 - \sum_{i=1}^{m} \left(Pi^2 \right)$$

Units: None.

Range: $0 \le SIDI < 1$.

SIDI = 0 when the landscape contains only 1 patch (no diversity). SIDI approaches 1 as the number of different patch types (patch richness, PR) increases and the proportional distribution of area among patch types becomes more equitable.

Description: SIDI equals 1 minus the sum, across all patch types, of the proportional abundance of each patch type squared.

Appendix B.4. Contag Index

Raster

$$CONTAG = \left(1 + \frac{\sum_{i=1}^{m} \sum_{i=1}^{m} \left[(P_i) \left(\frac{g_{ik}}{\sum_{k=1}^{m} g_{ik}} \right) \right] o \left[\ln(P_i) \left(\frac{g_{ik}}{\sum_{k=1}^{m} g_{ik}} \right) \right]}{2 \ln(m)} \right) (100)$$

Units: Percent.

Range: $0 < CONTAG \le 100$.

CONTAG approaches 0 when the distribution of adjacencies (at the level of individual cells) among unique patch types becomes increasingly uneven. CONTAG = 100 when all patch types are equally adjacent to all other patch types (that is, maximum interspersion and juxtaposition). CONTAG is undefined and reported as "NA" in the "basename".full file and as a dot "." in the "basename".land file if the number of patch types is less than 2.

Description: CONTAG equals 1 plus the sum of the proportional abundance of each patch type multiplied by the number of adjacencies between cells of that patch type and all other patch types, multiplied by the logarithm of the same quantity, summed over each patch type; divided by 2 times the logarithm of the number of patch types; and multiplied by 100 (to convert to a percentage). In other words, it is the observed contagion over the maximum possible contagion for the given number of patch types. CONTAG considers all patch types present in an image, including any present in the landscape border, and considers like adjacencies (cells of a patch type adjacent to cells of the same type). All background edge segments are ignored, as are landscape boundary segments if a border is not provided, because adjacency information for these edge segments is not available.

Appendix B.5. Edge Density

Vector/Raster

$$ED = \frac{E}{A}(10,000)$$

Units: Meters per hectare. Range: $ED \ge 0$, without limit.

ED = 0 when there is no edge in the landscape, that is, when the entire landscape and landscape border, if present, consists of a single patch and the user specifies that none of the landscape boundary and background edge be treated as an edge.

Description: ED equals the sum of the lengths (m) of all edge segments in the landscape, divided by the total landscape area (m²), multiplied by 10,000 (to convert to hectares). If

Land **2025**, 14, 2127 27 of 29

a landscape border is present, ED includes landscape boundary segments representing a true edge only (that is, contrast weight 0). If a landscape border is absent, ED includes a user-specified proportion of the landscape boundary. Regardless of whether a landscape border is present or not, ED includes a user-specified proportion of background edge Cited from McGarigal and Marks [35].

References

- 1. Gündüz, H.I. Land-Use Land-Cover Dynamics and Future Projections using GEE, ML, and QGIS-MOLUSCE: A case study in Manisa. *Sustainability* **2025**, *17*, 1363. [CrossRef]
- 2. Kundu, S.; Rana, N.K.; Mahato, S. Unravelling blue landscape fragmentation effects on ecosystem services in urban agglomerations. *Sustain. Cities Soc.* **2024**, *102*, 105192. [CrossRef]
- 3. Zhou, L.; Wei, L.; López-Carr, D.; Dang, X.; Yuan, B.; Yuan, Z. Identification of irregular extension features and fragmented spatial governance within urban fringe areas. *Appl. Geogr.* **2024**, *162*, 103172. [CrossRef]
- 4. van den Brandeler, F.; Gupta, J.; Hordijk, M. Megacities and rivers: Scalar mismatches between urban water management and river basin management. *J. Hydrol.* **2019**, *573*, 1067–1074. [CrossRef]
- 5. Taylor, M.S.; Wheeler, B.W.; White, M.P.; Economou, T.; Osborne, N.J. Research note: Urban street tree density and antidepressant prescription rates—A cross-sectional study in London, UK. *Landsc. Urban Plan.* **2015**, *136*, 174–179. [CrossRef]
- 6. Upreti, M.; Kumar, A. Landscape modeling for urban growth characterization and its impact on ecological infrastructure in Delhi-NCR: An approach to achieve SDGs. *Phys. Chem. Earth Parts A/B/C* **2023**, *131*, 103444. [CrossRef]
- 7. Vich, G.; Marquet, O.; Miralles-Guasch, C. Green streetscape and walking: Exploring active mobility patterns in dense and compact cities. *J. Transp. Health* **2019**, *12*, 50–59. [CrossRef]
- 8. Fahrig, L. Effects of Habitat Fragmentation on Biodiversity. Annu. Rev. Ecol. Evol. Syst. 2003, 34, 487–515. [CrossRef]
- 9. Mitchell, M.; Suarez-Castro, A.; Martinez-Harms, M.; Maron, M.; McAlpine, C.; Gaston, K.; Johansen, K.; Rhodes, J.R. Reframing landscape fragmentation's effects on ecosystem services. *Trends Ecol. Evol.* **2015**, *30*, 190–198. [CrossRef]
- 10. Pu, J.; Shen, A.; Liu, C.; Wen, B. Impacts of ecological land fragmentation on habitat quality in the Taihu Lake basin in Jiangsu Province, China. *Ecol. Indic.* **2024**, *158*, 111611. [CrossRef]
- 11. Diniz, É.S.; Mota, P.H.S.; Reis, J.P.; da Silva Costa, W.; de Paiva, E.V.; de Lana, J.M.; Lage, G.B.; do Amaral, C.H. Connectivity value of Atlantic forest fragments: Pathways towards enhancing biodiversity conservation. *Braz. J. Bot.* **2023**, 47, 249–259. [CrossRef]
- 12. Comino, E.; Bottero, M.; Pomarico, S.; Rosso, M. Exploring the environmental value of ecosystem services for a river basin through a spatial multicriteria analysis. *Land Use Policy* **2014**, *36*, 381–395. [CrossRef]
- 13. Peng, J.; Liu, S.; Lu, W.; Liu, M.; Feng, S.; Cong, P. Continuous Change Mapping to Understand Wetland Quantity and Quality Evolution and Driving Forces: A Case Study in the Liao River Estuary from 1986 to 2018. *Remote Sens.* 2021, 13, 4900. [CrossRef]
- 14. Aminzadeh, B.; Khansefid, M. A case study of urban ecological networks and a sustainable city: Tehran's metropolitan area. *Urban Ecosyst.* **2009**, *13*, 23–36. [CrossRef]
- 15. Rodriguez-Iturbe, I.; Muneepeerakul, R.; Bertuzzo, E.; Levin, S.A.; Rinaldo, A. River networks as ecological corridors: A complex systems perspective for integrating hydrologic, geomorphologic, and ecologic dynamics. *Water Resour. Res.* **2009**, *45*, W01413. [CrossRef]
- 16. Boquet, Y. Sustainable Urbanization in Southeast Asian Megacities: The Contrasting Cases of Singapore and Manila. In *Urban Dynamics, Environment and Health*; Sinha, B.R.K., Ed.; Springer: Singapore, 2023.
- 17. Chanieabate, M.; He, H.; Guo, C.; Abrahamgeremew, B.; Huang, Y. Examining the Relationship between Transportation Infrastructure, Urbanization Level and Rural-Urban Income Gap in China. *Sustainability* **2023**, *15*, 8410. [CrossRef]
- 18. Li, W.; Zinda, J.A.; Zhang, Z. Does the "Returning Farmland to Forest Program" Drive Community-Level Changes in Landscape Patterns in China? *Forests* **2019**, *10*, 933. [CrossRef]
- 19. Morichi, S. Long-Term Strategy for Transport System in Asian Megacities. J. East. Asia Soc. Transp. Stud. 2005, 6, 1–22.
- 20. Rahman, M.; Upaul, S.; Thill, J.-C.; Rahman, M. Active transportation and the built environment of a mid-size global south city. *Sustain. Cities Soc.* **2023**, *89*, 104329. [CrossRef]
- 21. Sánchez-Fernández, M.; Barrigón Morillas, J.M.; Montes González, D.; de Sanjosé Blasco, J.J. Impact of Roads on Environmental Protected Areas: Analysis and Comparison of Metrics for Assessing Habitat Fragmentation. *Land* **2022**, *11*, 1843. [CrossRef]
- 22. Ding, G.; Guo, J.; Ou, M.; Prishchepov, A.V. Understanding habitat isolation in the context of construction land expansion using an ecological network approach. *Landsc. Ecol.* **2024**, *39*, 56. [CrossRef]
- 23. Mohammadi, A.; Fatemizadeh, F. Quantifying landscape degradation following construction of a highway using landscape metrics in southern Iran. *Front. Ecol. Evol.* **2021**, *9*, 721313. [CrossRef]
- 24. Yirigui, Y.; Lee, S.; Nejadhashemi, A.P. Multi-Scale Assessment of Relationships between Fragmentation of Riparian Forests and Biological Conditions in Streams. *Sustainability* **2019**, *11*, 5060. [CrossRef]

Land 2025, 14, 2127 28 of 29

25. Dutta, A.; Dey, H. Assessing urban expansion and forest fragmentation in Dhaka Megacity using remote sensing and landscape metrics. *Acadlore Trans. Geosci.* **2024**, *3*, 210–220. [CrossRef]

- 26. Struebig, M.J.; Lee, J.S.H.; Deere, N.J.; Gevaña, D.T.; Ingram, D.J.; Lwin, N.; Nguyen, T.; Santika, T.; Seaman, D.J.; Supriatna, J.; et al. Drivers and solutions to Southeast Asia's biodiversity crisis. *Nat. Rev. Biodivers.* 2025, 1, 497–514. [CrossRef]
- 27. Robinson, N.; Allred, B.; Jones, M.; Moreno, A.; Kimball, J.; Naugle, D.; Erickson, T.; Richardson, A. A dynamic Landsat derived Normalized Difference Vegetation Index (NDVI) product for the conterminous United States. *Remote Sens.* **2017**, *9*, 863. [CrossRef]
- 28. Zou, L.; Wang, J.; Bai, M. Assessing spatial–temporal heterogeneity of China's landscape fragmentation in 1980–2020. *Ecol. Indic.* **2022**, *136*, 108654. [CrossRef]
- 29. Kurnianti, D.N.; Rustiadi, E.; Baskoro, D.P.T. Land use projection for spatial plan consistency in Jabodetabek. *Indones. J. Geogr.* **2015**, *47*, 124. [CrossRef]
- 30. Younger, J.S. Development of road infrastructure in Indonesia. Proc. Inst. Civ. Eng.—Munic. Eng. 2013, 166, 167–174. [CrossRef]
- 31. Richardson, M.; Soloviev, M. The Urban River Syndrome: Achieving sustainability against a backdrop of accelerating change. *Int. J. Environ. Res. Public Health* **2021**, *18*, 6406. [CrossRef]
- 32. Xu, X.; Zhu, G.; Zhang, C.; Zhao, X.; Li, Y. Research Progress of the Impacts of Comprehensive Transportation Network on Territorial Spatial Development and Protection. *Land* **2024**, *13*, 479. [CrossRef]
- 33. Dias, T.C.; Silveira, L.F.; Pironkova, Z.I.; Francisco, M.R. Greening and browning trends in a tropical forest hotspot: Accounting for fragment size and vegetation indices. *Remote Sens. Appl. Soc. Environ.* **2022**, *26*, 100751. [CrossRef]
- 34. Meneses-Tovar, C.L. NDVI as indicator of degradation. Unasylva 2011, 62, 39-46.
- 35. McGarigal, K.; Marks, B.J. FRAGSTATS: Spatial Pattern Analysis Program for Quantifying Landscape Structure; General Technical Report PNW-GTR-351; USDA Forest Service: Portland, OR, USA, 1995.
- 36. Olson, D.M.; Dinerstein, E.; Wikramanayake, E.D.; Burgess, N.D.; Powell, G.V.N.; Underwood, E.C.; D'Amico, J.A.; Itoua, I.; Strand, H.E.; Morrison, J.C.; et al. Terrestrial ecoregions of the world: A new map of life on Earth. *BioScience* **2001**, *51*, 933–938. [CrossRef]
- 37. Nurwanda, A.; Honjo, T. Analysis of land use change and expansion of surface urban heat island in Bogor City by remote sensing. ISPRS Int. J. Geo-Inf. 2018, 7, 165. [CrossRef]
- 38. Jatayu, A.; Saizen, I.; Rustiadi, E.; Pribadi, D.O.; Juanda, B. Urban Form Dynamics and Modelling towards Sustainable Hinterland Development in North Cianjur, Jakarta–Bandung Mega-Urban Region. *Sustainability* **2022**, *14*, 907. [CrossRef]
- 39. Vicharnakorn, P.; Shrestha, R.; Nagai, M.; Salam, A.; Kiratiprayoon, S. Carbon stock assessment using remote sensing and forest inventory data in Savannakhet, Lao PDR. *Remote Sens.* **2014**, *6*, 5452–5479. [CrossRef]
- 40. Olmanson, L.G.; Bauer, M.E.; Brezonik, P.L. A 20-year Landsat water clarity census of Minnesota's 10,000 lakes. *Remote Sens. Environ.* 2008, 112, 4086–4097. [CrossRef]
- 41. Wang, Z.; Yao, W.; Tang, Q.; Liu, L.; Xiao, P.; Kong, X.; Zhang, P.; Shi, F.; Wang, Y. Continuous change detection of Forest/Grassland and cropland in the Loess Plateau of China using all available Landsat data. *Remote Sens.* **2018**, *10*, 1775. [CrossRef]
- 42. Liu, S.; Zhang, J.; Wang, L.; Ciais, P.; Zhang, J.; Penuelas, J.; Nath, B.; Jacquet, I.; Wu, X.; Ding, S.; et al. Mapping previously undetected trees reveals overlooked changes in pan-tropical tree cover. *Nat. Commun.* **2025**, *16*, 5561. [CrossRef]
- 43. Gupta, K.; Kumar, P.; Pathan, S.K.; Sharma, K.P. Urban Neighborhood Green Index—A measure of green spaces in urban areas. *Landsc. Urban Plan.* **2012**, 105, 325–335. [CrossRef]
- 44. Pettorelli, N. The Normalized Difference Vegetation Index; Oxford University Press: Cary, NC, USA, 2013.
- 45. Fahrig, L. Patch-scale edge effects do not indicate landscape-scale fragmentation effects. Conserv. Lett. 2023, 17, e12992. [CrossRef]
- 46. Filigheddu, M.R.; Cillara, M.; Deplano, G.; Molgora, J.E.; Lai, L.; Muru, D.; Schirru, M.; Sedda, L.; Dettori, S. Analysis of land-use change in Mandrolisai 1860 to 2016: A case study from Sardinia (Italy). *Landsc. Hist.* **2024**, *45*, 81–100. [CrossRef]
- 47. Deere, N.J.; Bicknell, J.E.; Mitchell, S.L.; Afendy, A.; Baking, E.L.; Bernard, H.; Chung, A.Y.; Ewers, R.M.; Heroin, H.; Joseph, N.; et al. Riparian buffers can help mitigate biodiversity declines in oil palm agriculture. *Front. Ecol. Environ.* **2022**, *20*, 459–466. [CrossRef]
- 48. Putri, N.A. Rainfall maps for the suitability of settlement area in Bogor Raya. EnviroScienteae 2023, 19, 123–129. [CrossRef]
- 49. Marwasta, D. Spatial Trends of Urban Physical Growth of Cities in Java, Indonesia, 1975–2015. *ASEAN J. Sci. Technol. Dev.* **2019**, 36, 5. [CrossRef]
- 50. Fachrul, M.F.; Hendrawan, D.; Sitawati, A. Land use and water quality relationships in the Ciliwung river basin Indonesia. In Proceedings of the International Congress River Basin Management, Antalya, Turkey, 22–24 March 2007.
- 51. Pribadi, D.O.; Pauleit, S. The dynamics of peri-urban agriculture during rapid urbanization of Jabodetabek Metropolitan Area. *Land Use Policy* **2015**, *48*, 13–24. [CrossRef]
- 52. Sumarga, E.; Sholihah, A.; Srigati, F.A.; Nabila, S.; Azzahra, P.R.; Rabbani, N.P. Quantification of Ecosystem Services from Urban Mangrove Forest: A Case Study in Angke Kapuk Jakarta. *Forests* **2023**, *14*, 1796. [CrossRef]

Land 2025, 14, 2127 29 of 29

53. Kurniawan, T.A.; Meidiana, C.; Goh, H.H.; Zhang, D.; Jiang, M.; Othman, M.H.; Anouzla, A.; Aziz, F.; Mahmoud, M.; Khan, M.I.; et al. Social dimensions of climate-induced flooding in Jakarta (Indonesia): The role of non-point source pollution. *Water Environ. Res.* **2024**, *96*, e11129. [CrossRef]

- 54. Forman, R.T.T. Land Mosaics: The Ecology of Landscapes and Regions; Cambridge University Press: Cambridge, UK, 1995.
- 55. Huston, M.A. A general hypothesis of species diversity. Am. Nat. 1979, 113, 81-101. [CrossRef]
- 56. Naiman, R.J.; Décamps, H.; McClain, M.E. *Riparia: Ecology, Conservation, and Management of Streamside Communities*; Elsevier Academic Press: Cambridge, MA, USA, 2005.
- 57. Newton, A.; Mistri, M.; Pérez-Ruzafa, A.; Reizopoulou, S. Editorial: Ecosystem services, biodiversity, and water quality in transitional ecosystems. *Front. Ecol. Evol.* **2023**, *11*, 1136750. [CrossRef]
- 58. Heeres, N.; Van Dijk, T.; Arts, J.; Tillema, T. Coping with functional interrelatedness and stakeholder fragmentation in planning at the infrastructure-land use interface: The potential merits of a design approach. *J. Transp. Land Use* **2016**, *10*, 409–435. [CrossRef]
- 59. Laurance, W.F.; Bierregaard, R.O. *Tropical Forest Remnants: Ecology, Management, and Conservation of Fragmented Communities*; University of Chicago Press: Chicago, IL, USA, 1997.
- 60. Goosem, M. Linear infrastructure in the tropical rainforests of far north Queensland: Mitigating impacts on fauna of roads and powerline clearings. In *Conservation of Australia's Forest Fauna*; Royal Zoological Society of New South Wales: Mosman, Australia, 2004; pp. 418–434.
- 61. Riitters, K.H.; Wickham, J.D.; O'Neill, R.V.; Jones, K.B.; Smith, E. Global-scale patterns of forest fragmentation. *Conserv. Ecol.* **2000**, 4, 3. [CrossRef]
- 62. Hoffmeister, T.S.; Vet, L.E.; Biere, A.; Holsinger, K.; Filser, J. Ecological and evolutionary consequences of biological invasion and habitat fragmentation. *Ecosystems* **2005**, *8*, 657–667. [CrossRef]
- 63. Mustelier, D.; Henríquez, C. Modeling land use change of mid-sized cities in the process of metropolization. Case study La Serena-Coquimbo conurbation, Chile. *Geogr. Environ. Sustain.* **2024**, *17*, 106–118. [CrossRef]
- 64. Heeres, N.; Tillema, T.; Arts, J. Dealing with interrelatedness and fragmentation in road infrastructure planning: An analysis of integrated approaches throughout the planning process in the Netherlands. *Plan. Theory Pract.* **2016**, *17*, 421–443. [CrossRef]
- 65. Hilty, J.A.; Lidicker, W.Z.; Merenlender, A.M. Corridor Ecology: The Science and Practice of Linking Landscapes for Biodiversity Conservation; Island Press: Washington, DC, USA, 2006.

Disclaimer/Publisher's Note: The statements, opinions and data contained in all publications are solely those of the individual author(s) and contributor(s) and not of MDPI and/or the editor(s). MDPI and/or the editor(s) disclaim responsibility for any injury to people or property resulting from any ideas, methods, instructions or products referred to in the content.